PHYSICAL REVIEW B VOLUME 26, NUMBER 8 15 OCTOBER 1982

Lattice dynamics of mixed alkali halides. I. Negative-ion substitution

Néstor E. Massa
Behlen Laboratory of Physics, University of Nebraska, Lincoln, Nebraska 68588

Shashanka S. Mitra
Electrical Engineering Department, University of Rhode Island, Kingston, Rhode Island 02881

John F. Vetelino
Electrical Engineering Department, University of Maine, Orono, Maine 04469
(Received 23 January 1981; revised manuscript received 11 December 1981)

Phonon frequencies of one-mode behavior of mixed alkali-halide crystals with negative-ion substitution have been calculated as a function of wave-vector and molar-mixing ratio. The mixed-crystal model utilizes a pseudo-unit-cell as a basic repetitive unit incorporated into the breathing-shell model of lattice dynamics. The fundamental repetitive unit cell for the mixed crystal $AB_{1-x}C_x$ consists of A ions at their normal lattice site and with nearest neighbors consisting of a fractional amount of B and C ions proportional to their mixing molar ratio. The model parameters are deduced from physical observables such as the elastic constants, long-wavelength transverse-optical mode frequency, and the high- and low-frequency dielectric constants of the parent compounds. Room-temperature calculations of one- and two-phonon densities of states and dispersion relations of $KCl_{1-x}Br_x$, $KCl_{1-x}I_x$, and $KBr_{1-x}I_x$ are found to agree with the available Raman scattering, infrared reflection, and absorption data.

I. INTRODUCTION

A solid may be considered as an ordered or disordered system depending on whether its atomic arrangement is a lattice or not, corresponding to the ideal crystalline and amorphous states, respectively. Mixed crystals, on the other hand, may be regarded as solid solutions in which the crystalline lattice topology is preserved but in which the atomic spatial arrangements depend on the molar concentration of impurity atoms in the host crystal. Thus, they may be considered a particular case of disordered systems marked by a close association with the dynamics of the perfect crystal but lacking in translational periodicity.

The determination of the vibrational properties of mixed crystalline compounds will be based on the assumption that the nature of the disorder is such that its properties can be obtained as an appropriate extension of the corresponding properties of the ideal ordered system. As the impurity content increases, it changes from playing a localized role in the frequency spectrum to one comparable to that of the host system. In this case the compound is called a mixed crystal.

From the x-ray point of view, the system formed by the mixture of pure compounds is truly a crystalline formation. The latter displays unique lattice constants that change linearly with the molar concentration (Vegard's law[1]) from one pure end member to the other. Disorder is configurational in contrast to glasses in which it is also spatial.

Localized impurity ions that only break the translational and inversion symmetries will be considered as limits for very low molar concentration and they will be discussed only in the framework of mixed-crystal systems. In particular, our interest will be limited to mixed alkali-halide compounds. For the pure end members of such systems the breathing-shell model[2] is known to apply well.

Experimentally, mainly through far-infrared and Raman spectroscopy, it is observed that when two pure alkali halides are mixed by substituting for a cation or an anion two extreme situations can occur: In one case only one set of long-wavelength phonons will be evident, characteristic of the resultant system at any molar concentration. In the other case, an equally typical behavior, two sets of frequencies appear, i.e., a longitudinal-optical (LO_1) and a transverse-optical (TO_1) mode associated with one end-member diatomic compound and a longitudinal-optical (LO_2) and a transverse-optical (TO_2) mode corresponding to the other end-

member diatomic compound. These two behavior types are known in the literature as one-mode and two-mode behavior. A review of the experimental data as well as the models has been given by Chang and Mitra.[3] Barker and Sievers[4] have made an extensive review of lattice vibrations associated with defects, emphasizing the infrared absorption and Raman scattering spectra.

Based on the idea that the appearance of two reststrahlen bands may be thought of as consequence that the two mixing components in $AB_{1-x}C_x$ are in sublattices that vibrate rather independently against the lattice of the nonmixing ion sublattice, Chen *et al.*[5] proposed their random-element-isodisplacement (REI) model. They assumed that the cation and anion of the like species form units that vibrate with the same phase and amplitude. The important factor in this model is that force constants F_{AB},F_{AC} between ions A and B, and A and C, change linearly with concentration as do the lattice constant. However, the force constant F_{BC} is a fitting parameter whose value is chosen to obtain a very good agreement with the experimental results for $GaP_{1-x}As_x$. A step forward had been achieved by Chang and Mitra[6] by modifying the REI model (MREI) so that it includes the Coulomb field. The result of employing this field is that the model reproduces the known long-wavelength frequencies of the end member crystals AB and AC. With these boundary conditions F_{BC} is calculated. The MREI model is able to predict the zone-center frequencies for any molar concentration for two-mode and one-mode behavior systems, and it has been extended by Genzel *et al.*[7] to develop a series of relations for predicting the appearance of one- and two-mode behavior from the character of the pure compounds. These were later modified by other authors[8–10] and must be considered only as useful guides.

A more recent attempt to describe the lattice dynamics of mixed crystals was made by Kutty[11] using the Green's-function technique. Tripathi and Behera,[12] by means of a Green's-function formulation, proposed a self-consistency theory for phonons in mixed crystals without conclusive results. The coherent-potential approximation[13] (CPA) must also be mentioned as a potentially useful approach to study disordered systems. In particular, the work of Taylor should be cited[14] in which CPA technique leads to some success in three-dimensional calculations of the spectral features of mixed alkali halides. Sen and Hartmann[15] used the coherent approximation to explain the switching from one-mode to two-mode behavior in one dimension.

Chang and Mitra,[6,16] beginning with the concept that the mixed-crystal behavior must follow the pattern of the pure end members developed the concept of the pseudo-unit-cell to explain the zone-center phonons at any concentration. It is assumed that mixing atoms are randomly distributed and that the components of the unit cell are defined as A, $(1-x)B$, and xC, $(0 \leq x \leq 1)$ where B and C are the substituting ions. The force on ion A due to ion B is given by $(1-x)F_{AB}$, due to ion C by xF_{AC}, but the force exercised on B due to A is F_{AB} and the one on C due to A is F_{AC} because the molar fraction of ion A is one. The generalized equations of motion in a one-dimensional mixed diatomic unit cell were proposed by Vetelino and Mitra.[17] Varshney *et al.*[18] have calculated the lattice dynamics of $ZnS_{1-x}Se_x$ and $GaP_{1-x}As_x$ using the pseudo-unit-cell model and the coupling coefficients of the rigid-ion model of lattice dynamics affected by molar-concentration factors. Twelve constants are calculated from physical observables. However, to fill the gap between the experimental data and the unknown input a fitting in the least-squares sense is introduced that results in an elaborate procedure with no immediate physical interpretation, thus precluding the generalization of the method.

Our idea consists of attacking the problem on a broader basis by extending the two-dimensional pseudo-unit-cell concept to a three-dimensional analysis for an $AB_{1-x}C_x$ mixed system. In the present approach previous nonphysical assumptions such as those of force constants that vary with concentration in a linear functional form by the introduction of a parameter θx (Refs. 6, 16, 18, and 19) and the least-squares fit used to determine model parameters of the mixed system[20] are dropped. It is shown that the knowledge of the model parameters of the pure end members and the assumption that force constants, as well as lattice constants, vary linearly from one pure end member to the other is sufficient to describe the lattice dynamics of a mixed alkali-halide crystal.

II. BREATHING MIXED-DIATOMIC LINEAR CHAIN

The picture of a breathing mixed-diatomic linear chain will be presented here to point out the basic

ideas in the development of the three-dimensional model presented later and to avoid the lengthy algebra that is involved in deducing explicitly the three-dimensional coupling coefficients. Figure 1(a) shows a mixed linear chain for the $A^+B^-_{1-x}C^-_x$ system with only nearest-neighbor interactions with a negative effective ion that is "breathing." Second-neighbor interactions are shown in Fig. 1(b). We do not agree with the *ad hoc* assumption that one-mode behavior may be explained in terms of a resonant mode associated with the C_x impurity in a AB_{1-x} host crystal with $x \simeq 0$ and that such resonant behavior could be extended to any concentration x. This is questionable in that this situation may be predictable in an almost pure compound but we believe it is unphysical to propose it for polar crystals at finite concentrations, since one would expect the development of a macroscopic field associated with each set of vibrational modes. At long wavelengths this would show in infrared as an extra reststrahlen band due to the "impurity" LO-TO splitting in addition to the "one-mode" band. This description is close to what arises in a two-mode compound as it is known for $K_{x-1}Rb_xI$,[9] and, more recently, in $K_{1-x}Tl_xCl$ and $K_{1-x}Tl_xBr$.[20] These systems, at $x=0$ and $x=1$, and in the long-wavelength limit, have a spectrum that reduces to a band related to the host crystal accompanied by a local mode.

For these reasons we have focused our attention on the force-constant behavior for the first and second neighbors, and watching for the set that will produce what is experimentally known. Below, one-dimensional equations of motion abstracted from the actual three-dimensional problem for one behavior are written. These are written in terms common to the three-dimensional cases, i.e., u's are the core displacements, v's are the shell-core displacements, and r's are the shell deformations. The pseudocell is assumed to contain either two "hard" or "soft" atoms constituting the "pseudo-mixing-ion" and a third ion as is shown in Fig. 1(a). The figures take into account the interaction of the i and j ions. Hence the equations for one-mode behavior $A^+B_{1-x}C^-_x$ system with B^-_{1-x} and C^-_x breathing (e.g., $KCl_{1-x}Br_x$) written with Bilz's notation for the one-dimensional-shell model[21] become core equations,

$$
\begin{aligned}
m^A\ddot{u}^A_{2n} &= (1-x)F_{AB}(v^B_{2n+1}+v^B_{2n-1}-2u^A_{2n})+xF_{AC}(v^C_{2n+1}+v^C_{2n-1}-2u^A_{2n}) \\
&\quad +F_{AA}(u^A_{2n+2}-2u^A_{2n}+u^A_{2n-2})\,, \\
(1-x)m^B\ddot{u}^B_{2n-1} &= (1-x)k_B(u^B_{2n-1}-v^B_{2n-1})\,, \\
xm^C\ddot{u}^C_{2n-1} &= xk_C(u^C_{n-1}-v^C_{2n-1})\,,
\end{aligned}
\tag{2.1a}
$$

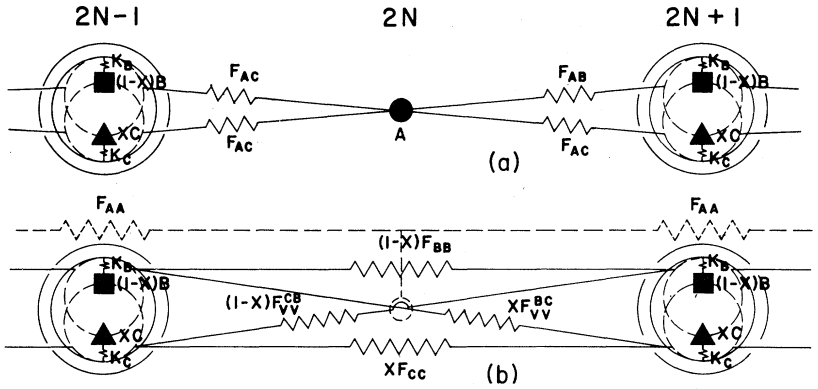

FIG. 1. Mixed diatomic linear chain: (a) Nearest- neighbor interactions, (b) second-neighbor interactions (one-mode behavior).

shell equations,

$$
\begin{aligned}
0=&(1-x)k_B(v^B_{2n-1}-u^B_{2n-1})+(1-x)f_{AB}(2v^B_{2n-1}-u^A_{2n-2}-u^A_{2n})\\
&+(1-x)^2F_{BB}(2v^B_{2n-1}-v^B_{2n-3}-v^B_{2n+1})+x(1-x)F^{BC}_{vv}(2v^B_{2n-1}-v^C_{2n-3}-v^C_{2n+1})\\
&+x(1-x)F_{AC}\Delta r_C+(1-x)^2F_{AB}\Delta r_B\ ,\\
0=&xk_C(v^C_{2n-1}-u^C_{2n-1})+xf_{AC}(2v^C_{2n-1}-u^A_{2n-2}-u^A_{2n})\\
&+x^2F_{CC}(2v^C_{2n-1}-v^C_{2n-3}-v^C_{2n+1})+(1-x)f^{CB}_{vv}(2v^C_{2n-1}-v^B_{2n-3}-v^B_{2n+1})\\
&+x(1-x)F_{AB}\Delta r_B+x^2F_{AC}\Delta r_C\ ,
\end{aligned}
\tag{2.1b}
$$

and "breathing" equations,

$$
\begin{aligned}
&F_{AB}(2v^B_{2n-1}-u^A_{2n}-u^A_{2n-2})\\
&\quad+H_{AB}\Delta r_B+H_{BC}\Delta r_C=0\ ,\\
&F_{AC}(2v^C_{2n-1}-u^A_{2n}-u^A_{2n-2})\\
&\quad+H_{AC}\Delta r_C+H_{CB}\Delta r_B=0\ ,
\end{aligned}
\tag{2.1c}
$$

where $H=2F_{Ah}+G$ $(h=B,c)$ and m^N $(N=A,B,C)$ are the ion masses. It can be observed that the force constants are multiplied by molar weights that correspond to the presence of the ion in the pseudo-unit-cell. Besides, the masses of the substituting ions are weighted by their concentration, as shown in Fig. 1. Naturally, in the three-dimensional picture only one particle is on each lattice site and no first-neighbor interactions are allowed between like charge atoms since this would imply the explicit introduction of the idea of unstability in the mixed compound.[19] The two molar mass factors imply a net molar dependence for each term of the dynamical matrix that will affect the coupling coefficients shown in the following sections.

III. THE THREE-DIMENSIONAL PSEUDO-UNIT-CELL APPROACH

The three-dimensional model that uses the breathing-shell model[22] of lattice dynamics, known to give a reliable description of the neutron scattering data on pure alkali-halide crystals, considers nearest neighbors and next-nearest neighbors for effective negative-ion–negative-ion interactions. In principle, the equation of motion involving ion displacements for $A^+B^-_{1-x}C^-_x$ can be described by

$$
\underline{M}\begin{pmatrix}\ddot{U}_{A^+}\\ \ddot{U}_{B^-_{1-x}}\\ \ddot{U}_{C^-_x}\end{pmatrix}=\begin{pmatrix}A^+A^+ & A^+B^-_{1-x} & A^+C^-_x\\ B^-_{1-x}A^+ & B^-_{1-x}B^-_{1-x} & B^-_{1-x}C^-_x\\ C^-_xA^+ & C^-_xB^-_{1-x} & C^-_xD^-_x\end{pmatrix}\begin{pmatrix}U_{A^+}\\ U_{B^-_{1-x}}\\ U_{C^-_x}\end{pmatrix}\ ,
\tag{3.1}
$$

where $\underline{M}$ is the diagonal matrix specifying the effective masses, U_i is the column Cartesian displacement matrix for the three ions $(i=A^+, B^-_{1-x}, C^-_x)$. A^+A^+, $A^+B^-_{1-x}$, etc., are matrices that take into account short- and long-range interactions, polarization and breathing effects between ions A^+A^+, $A^+B^-_{1-x}$, etc. The superscript means the charge of the ion and the subscript the molar-concentration dependence. This, in terms of the BSM, implies that the dynamical problem is still described by the equation

$$
\begin{aligned}
\underline{M}\omega^2\underline{U}=&[\underline{R}+\underline{Z}\,\underline{C}\,\underline{Z}-(\underline{R}+\underline{Z}\,\underline{C}\,\underline{Y}-\underline{Q}\underline{H}^{-1}\underline{Q}^+)(\underline{R}+\underline{K}+\underline{Y}\,\underline{C}\,\underline{Y}-\underline{Q}\underline{H}^{-1}\underline{Q}^+)^{-1}(\underline{R}+\underline{Y}\,\underline{C}\,\underline{Z}-\underline{Q}\underline{H}^{-1}\underline{Q}^+)\\
&-\underline{Q}\underline{H}^{-1}\underline{Q}^+]\underline{U}\ ,
\end{aligned}
\tag{3.2}
$$

where short-range coupling coefficients ($\underline{R}$), Coulomb ($\underline{C}$), atom-shell deformation ($\underline{Q}$), shell-deformation–shell-deformation ($\underline{H}$) interactions, and the diagonal matrices for the effective masses ($\underline{M}$), ionic charges ($\underline{Z}$), shell charges ($\underline{Y}$), and core with own shell interaction ($\underline{K}$) are now 9×9 matrices due to the presence of three ions in the pseudo-unit-cell. As in the linear case, first-nearest

neighbor and second-negative-neighbor interactions are being considered as in the modified random-element-isodisplacement model (MREI), i.e., there are $(1-x)B$ ions and xC ions nearest neighbors to A, and no first-neighbors interactions are allowed between like charge ions. The only inputs used are the macroscopic physical properties like elastic constants C_{11}, C_{12}, C_{44}, the long-wavelength transverse optical frequency (TO), and the high- and low-frequency dielectric constants of the two end-member compounds. In addition, the stability condition has been used.

One- and two-phonon densities of states have been calculated for 64 000 frequencies by weighting each multiplicity of the phonon frequencies of the optical band in the pseudo-Brillouin zone by the molar fraction associated to the compound end member to which it would belong.

The next sections are dedicated to explaining the cases experimentally studied for negative-ion substitution resulting in one-mode behavior. In spite of the lack of experimental data, two-phonon interactions have also been included, because they are helpful in explaining sideband spectra, very often detected and sometimes erroneously attributed to first-order modes, and to encourage spectroscopic research in this area.

IV. ONE-MODE BEHAVIOR MIXED CRYSTALS WITH NEGATIVE-ION SUBSTITUTION

A. Formulation of the problem and molar-dependence parameters

There are three alkali-halide mixed crystals which show one-mode behavior and which have been fairly well studied. They are namely, $KCl_{1-x}Br_x$, $KCl_{1-x}I_x$, $KBr_{1-x}I_x$.

Consistent with the one-dimensional approach, a positive-positive interaction must evolve from the pure compounds A^+B^- and A^+C^-. Then, since all the lattice dynamics are built upon a harmonic first-order calculation it seems logical that they mix linearly,

$$\begin{aligned} A &= A_{AB}(1-x)+A_{AC}x \ , \\ B &= B_{AB}(1-x)+B_{AC}x \ , \end{aligned} \tag{4.1}$$

where A,B are the nearest-neighbor force constants of the mixed system. The subscripts AB and AC refer to the diatomic parent crystals. Second-neighbor interactions between the positive ions are not explicitly considered. Consequently, the self-term can be written as

$$W_{K1} = -(A+2B) \ . \tag{4.2}$$

Physically, this approach implies that one may think of A^+ in terms of a virtual particle that will be identical to A^+ ion at the two extremes, $x=0$ and 1. The ionic charge associated with this "particle" will be also the linear combination of those of system A^+B^- and A^+C^-,

$$\begin{aligned} Z_A &= (1-x)Z_B + xZ_C \ , \\ Z_B &= Z_{AB}, \quad Z_C = Z_{AC} \ , \end{aligned} \tag{4.3}$$

where as before the subscripts characterize the parent compound. Besides, it is in agreement with the general idea that the model must reduce itself to reproduce the phonon spectra of the pure crystals when no impurity is present. The same idea is behind the force constants of the crossed second-neighbor negative-negative interaction, $B^-_{1-x} \rightarrow C^-_x$, i.e.,

$$A_{BC} = \sqrt{A_{AB}A_{AC}} \ , \tag{4.4}$$

$$B_{BC} = (-1)\sqrt{B_{AB}B_{AC}} \ ,$$

$$A'_{BC} = (1-x)A'_{AB} + xA'_{AC} \ , \tag{4.5}$$

$$B'_{BC} = (1-x)B'_{AB} + xB'_{AC} \ .$$

It is important to stress that here negative-negative interactions imply second-neighbor interactions in which the self-term is

$$W_{K23} = -(A_{BC} + 2B_{BC} + 2A'_{BC} + 4B'_{BC}) \ , \tag{4.6}$$

and that the core-shell restoring force constant will change linearly from k_B, of the B^- ion to k_C of the C^- ion. The breathing, and, because of the presence of two negative particles, the breathing-breathing interactions, will have to be defined in terms of another set of force constants. These are contained in relations similar to Eq. (2) of Ref. 22. Hence

$$\begin{aligned} A_{12} &= (1-x)A_{AB} \ , \\ A_{13} &= xA_{AC} \ , \end{aligned}$$

with H now rewritten as

$$\begin{aligned} H_{BB} &= 6A_B + G_{AB} \ , \\ H_{CC} &= 6A_C + G_{AC} \ , \\ H_{BC} &= A(\cos 2\pi q_x r_0 + \cos 2\pi q_y r_0 + \cos q_z r_0 2\pi) \ . \end{aligned} \tag{4.7}$$

The pseudo-unit-cell includes other force constants,

TABLE I. Short-range force constants and model parameters of $KCl_{1-x}Br_x$.

$x=$	0.000 01	0.05	0.25	0.45	0.65	0.95	0.999 99	Units
A_{AB}	10.898	10.898	10.898	10.898	10.898	10.898	10.898	$e^2/2v$
A_{AC}	11.241	11.241	11.241	11.241	11.241	11.241	11.242	$e^2/2v$
A	10.898	10.915	10.983	11.052	11.121	11.223	11.241	$e^2/2v$
B_{AB}	−0.8817	−0.8817	−0.8817	−0.8817	−0.8817	−0.8817	−0.8817	$e^2/2v$
B_{AC}	−0.8817	−0.8817	−0.8817	−0.8817	−0.8817	−0.8817	−0.8817	$e^2/2v$
B	−0.8817	−0.8817	−0.8817	−0.8817	−0.8817	−0.8817	−0.8817	$e^2/2v$
A'_{AB}	-0.3145×10^{-1}	-0.3145×10^{-1}	-0.3145×10^{-1}	-0.3145×10^{-1}	-0.1345×10^{-1}	-0.3145×10^{-1}	-0.1345×10^{-1}	$e^2/2v$
A'_{AC}	−0.1251	−0.1251	−0.1251	−0.1251	−0.1251	−0.1251	−0.1251	$e^2/2v$
A'	-0.3145×10^{-1}	-0.3613×10^{-1}	-0.5487×10^{-1}	-0.7361×10^{-1}	-0.9235×10^{-1}	−0.1204	−0.1251	$e^2/2v$
B'_{AB}	-0.5334×10^{-4}	-0.5334×10^{-4}	-0.5334×10^{-4}	-0.5334×10^{-4}	-0.5334×10^{-4}	-0.5334×10^{-4}	-0.5334×10^{-4}	$e^2/2v$
B'_{AC}	-0.5328×10^{-4}	-0.5328×10^{-4}	-0.5328×10^{-4}	-0.5328×10^{-4}	-0.5328×10^{-4}	-0.5328×10^{-4}	-0.5328×10^{-4}	$e^2/2v$
B'	-0.5334×10^{-4}	-0.5334×10^{-4}	-0.5333×10^{-4}	-0.5332×10^{-4}	-0.5331×10^{-4}	-0.5328×10^{-4}	-0.5328×10^{-4}	$e^2/2v$
Z_{AB}	0.87	0.87	0.87	0.87	0.87	0.87	0.87	e
Z_{AC}	0.87	0.87	0.87	0.87	0.87	0.87	0.87	e
Z	0.87	0.87	0.87	0.87	0.87	0.87	0.87	e
Y_{AB}	−6.76	−6.76	−6.76	−6.76	−6.76	−6.76	−6.76	e
Y_{AC}	−6.71	−6.71	−6.71	−6.71	−6.71	−6.71	−6.71	e
Y	−6.760	−6.757	−6.747	−6.737	−6.727	−6.712	−6.71	e
k_{AB}	1209.90	1209.90	1209.90	1209.90	1209.90	1209.90	1209.90	$e^2/2v$
k_{AC}	1044.81	1044.81	1044.81	1044.81	1044.81	1044.81	1044.81	$e^2/2v$
k	1209.90	1201.65	1268.63	1135.62	1102.60	1053.07	1044.81	$e^2/2v$
G_{AB}	4815.47	4815.47	4815.47	4815.47	4815.47	4815.47	4815.46	$e^2/2v$
G_{AC}	1311.62	1311.62	1311.62	1311.62	1311.62	1311.62	1311.62	$e^2/2v$

as such of a $A_+C^-_{1-x}$ interaction, but they are those of the pure end compounds.

B. Coupling coefficients

In this section the molar dependence of short-range interactions and Coulomb coefficients will be introduced in terms of the above force constants. Thus the positive-positive short-range interaction will be reduced to

$$R_{xx}(AA)=W_{K1}\ ,$$
$$R_{xy}(AA)=0\ . \tag{4.8}$$

Cyclic permutation of the coordinates generates the rest of the coefficients. In the following only these two terms will be stated. In the same way that the force constants of positive-positive interactions were considered to have their magnitude constant for any molar concentration, $B^-_{1-x}B^-_{1-x}$ and $C^-_xC^-_x$ coupling coefficients will be proportional to their molar concentration. Hence, second-neighbor short-range interactions R_{BB} will be given by

$$\begin{aligned}R_{xx}(BB)=&[W_{K2}+(A'_{AB}B'_{AB})\cos2\pi q_xr_0\\&\times(\cos2\pi q_yr_0+\cos2\pi q_zr_0)\\&+2B'_{AB}\cos2\pi q_yr_0\cos2\pi q_zr_0](1-x)\ ,\\R_{xy}(BB)=&[-(A'_{AB}-B'_{AB})\sin2\pi q_x\\&\times r_0\sin2\pi q_yr_0](1-x)\ ,\end{aligned} \tag{4.9}$$

with

$$W_{K2}=-(A_{AB}+2B_{AB}+2A'_{AB}+4B'_{AB})\ .$$

Similarly for $R_{CC'}$,

$$\begin{aligned}R_{xy}(CC)=&[W_{K3}+(A'_{AC}+B'_{AC})\cos2\pi q_xr_0\\&\times(\cos2\pi q_yr_0+\cos2\pi q_zr_0)\\&+2B'_{AC}\cos2\pi q_yr_0\cos2\pi q_zr_0]x\ ,\\R_{xy}(CC)=&[-(A'_{AC}-B'_{AC})\sin2\pi q_xr_0\\&\times\sin2\pi q_yr_0]x\ ,\end{aligned} \tag{4.10}$$

$$W_{K3}=-(A_{AC}+2B_{AC}+2A'_{AC}+4B'_{AC})\ ,$$

Next, it is necessary to take into account the nearest-neighbor interactions. These are easily treated in the context of how forces were made molar dependent in the linear pseudo-unit-cell:

$$\begin{aligned}R_{xx}(AB)=&[A_{AB}\cos2\pi q_xr_0\\&+B_{AB}(\cos2\pi q_yr_0+\cos2\pi q_zr_0)]\\&\times\sqrt{1-x}\ ,\\R_{xy}(AB)=&0\ .\end{aligned} \tag{4.11}$$

Similar reasoning leads to

$$\begin{aligned}R_{xx}(AC)=&[A_{AC}\cos2\pi q_xr_0\\&+B_{AC}(\cos2\pi q_yr_0+\cos2\pi q_zr_0)]\\&\times\sqrt{x}\ ,\\R_{xy}(AC)=&0\ ,\end{aligned} \tag{4.12}$$

where $(1-x)$ was replaced by x stressing that this interaction is complementary to the previous one. Analogously, for the $B^-_xC^-_{1-x}$ interactions, it is inferred that the R_{BC} matrix will be affected by $x(1-x)$. We have the following:

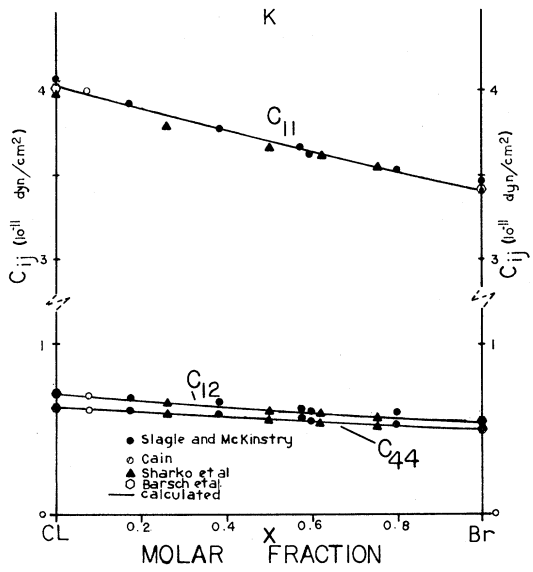

FIG. 2. Concentration dependence of the elastic constants of $KCl_{1-x}Br_x$.

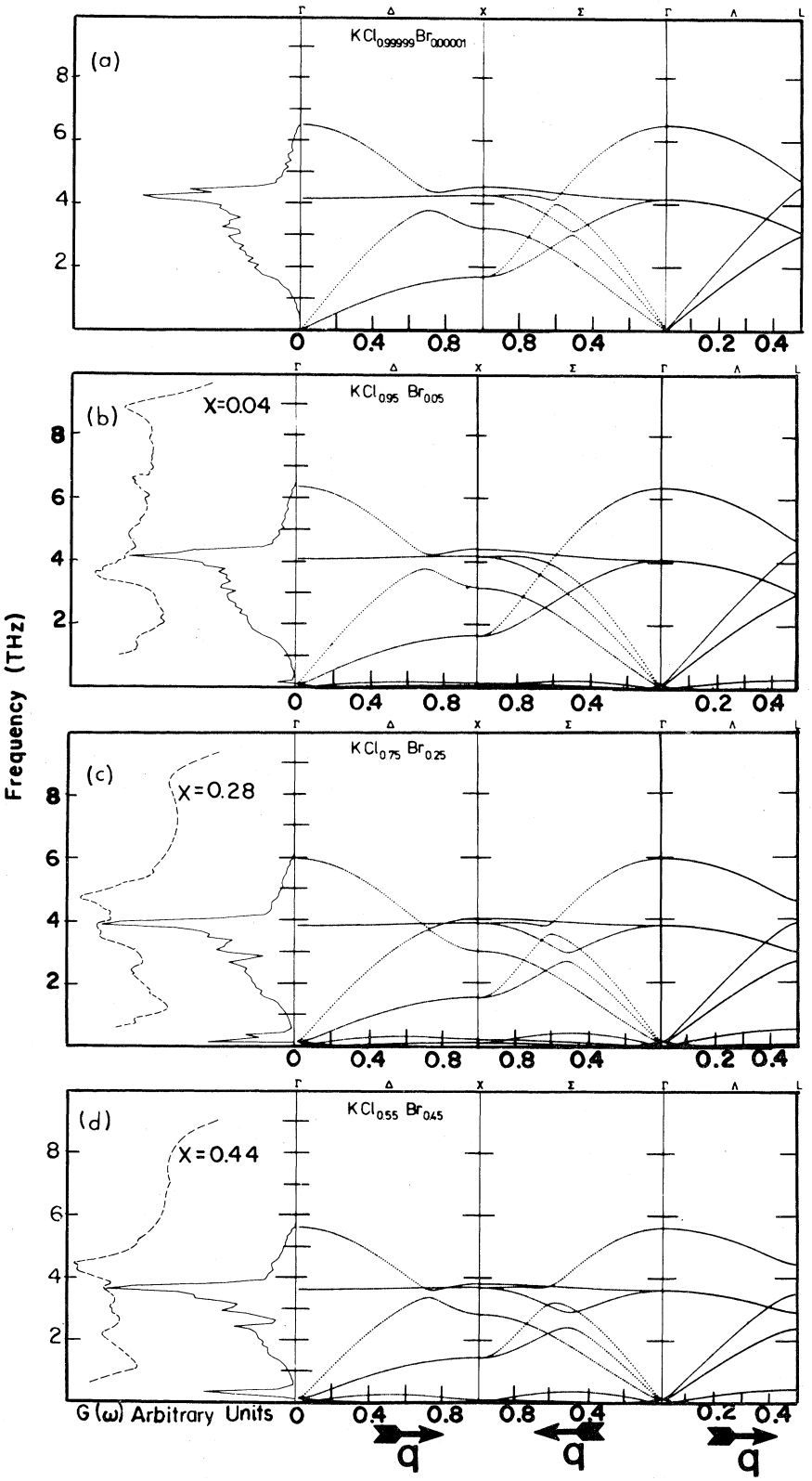

FIG. 3. One-phonon densities of states and dispersion relations for $KCl_{1-x}Br$. Dashed lines correspond to Raman scattering results from Ref. 25.

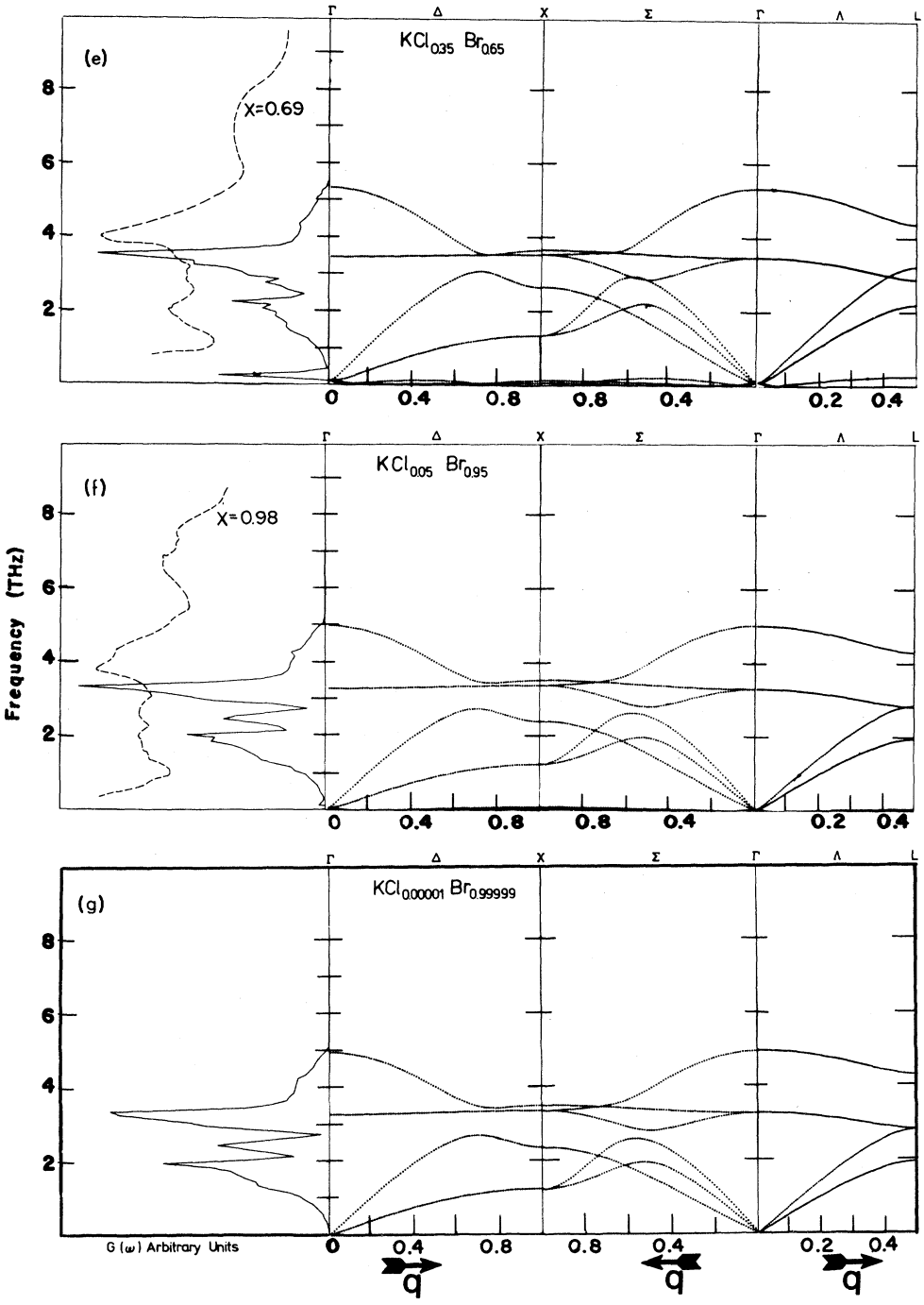

FIG. 3. (*Continued.*)

$$R_{xx}(BC)=[(W_{K23}+A'_{BC}+B'_{BC})\cos 2\pi q_x r_0(\cos 2\pi q_y r_0+\cos 2\pi q_z r_0)$$
$$+2B'_{BC}\cos 2\pi q_y r_0\cos 2\pi q_z r_0]\sqrt{x(1-x)}\,, \tag{4.13}$$
$$R_{xy}(BC)=[-(A'_{BC}-B'_{BC})\sin 2\pi q_x r_0\sin 2\pi q_y r_0]\sqrt{x(1-x)}\,.$$

Electrostatic interactions, treated separately and summed additive for the convenience of the calculation, will

be weighted by the same factors that were used for the short-range interaction. Explicitly, this means

$$C_{ij}(A,A)=C\begin{bmatrix}+ & +\\ i & j\end{bmatrix} \text{ for } C_{AA},\quad C_{ij}(A,B)=\sqrt{(1-x)}C\begin{bmatrix}+ & -\\ i & j\end{bmatrix} \text{ for } C_{AB},$$

$$C_{ij}(B,B)=C\begin{bmatrix}- & -\\ i & j\end{bmatrix}(1-x) \text{ for } C_{BB},\quad C_{ij}(A,C)=\sqrt{x}\,C\begin{bmatrix}+ & -\\ i & j\end{bmatrix} \text{ for } C_{AC},$$

$$C_{ij}(C,C)=C\begin{bmatrix}- & -\\ i & j\end{bmatrix}x \text{ for } C_{CC},\quad C_{ij}(B,C)=\sqrt{x(1-x)}C\begin{bmatrix}- & -\\ i & j\end{bmatrix} \text{ for } C_{BC},$$

$$\text{for all } i,j;x,y,z\ . \qquad (4.14)$$

Once the coupling coefficients are determined, the determinant is solved for ninety points along each principal direction of the pseudo-unit-cell in the reciprocal space. Impurities are expected to lift degeneracies present in the crystalline Brillouin zone. The densities of states are calculated by assuming that an eigenvalue at a particular symmetry point will have a multiplicity at the point directly proportional to the molar concentration of the diatomic compound associated with the phonon. Hence, by identifying each eigenvalue it is possible to associate it with the acoustical or optical bands before it enters in a channel and is counted. Those in the acoustical band will not be weighted. On the other hand, optical phonons will have a multiplicity concentration dependence as pointed out above. The same criterion was applied in calculating the two-phonon spectra in which the summation bands were correlated according to the weight of the first-order phonons intervening in the combination.

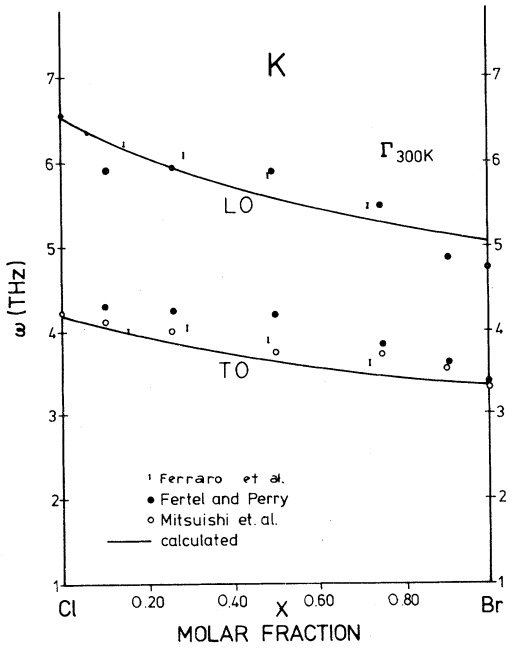

FIG. 4. Transverse- and longitudinal-optical modes of $KCl_{1-x}Br_x$.

C. Dispersion relations and density of states

1. $KCl_{1-x}Br_x$

Table I shows the force constants and the model parameters as evaluated to calculate the lattice dynamics. Elastic constants were measured by Slagle and McKinstry[23] and Sharko and Botaki,[24] corroborating the basic idea that for mixed alkali halides one may correctly assume a linear change of the force constants. These are compared with the calculated elastic constants in Fig. 2 and show excellent agreement. The infrared phonon spectra have been measured by Fertel and Perry[9]; the Raman spectra have been measured by Nair and Walker[25] and also by Fertel and Perry.[26] Ferraro *et al.*[27] measured the high-pressure spectra. Comparison of theoretical results with these data follows. Figures 3(a)—3(g) are the one-phonon spectra for 0.000 01, 0.05, 0.25, 0.45, 0.65, 0.95, and 0.999 99 molar fractions.

It is possible to see that the main features correspond to a reststrahlen band that moves nearly linearly from one end to the other, the acoustic band, and a low-lying band that fulfills the three extra degrees of freedom that are due to the third ion in the pseudo-unit-cell. On the left-hand side the Raman results from Ref. 25 are superimposed to the calculated density of states.

Low-lying modes show a narrow band that at low concentration does not disturb the phonon spectrum of the host crystal. As the impurity con-

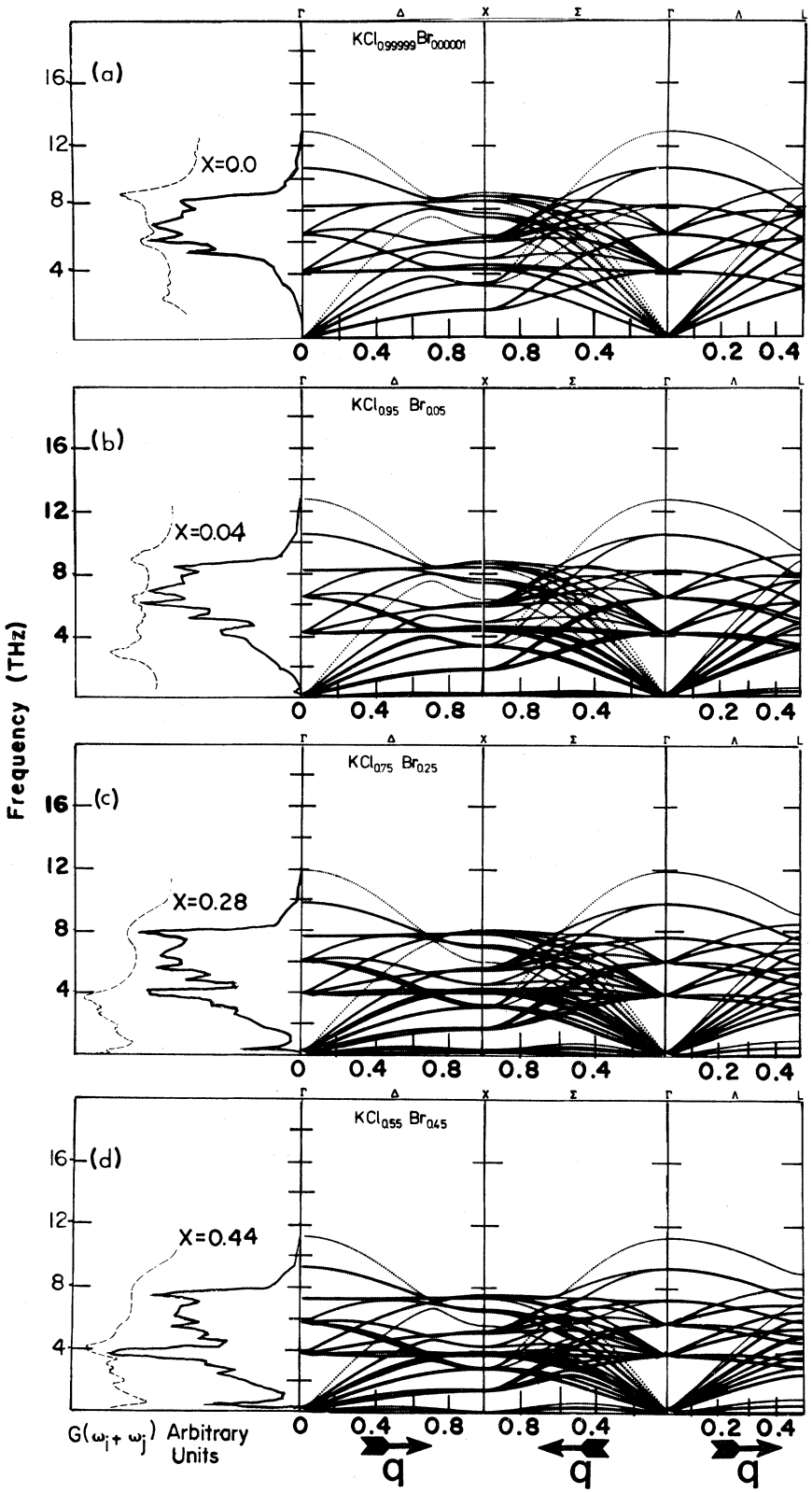

FIG. 5. Two-phonon densities of states and dispersion relations of $KCl_{1-x}Br_x$. Dashed lines correspond to Raman scattering results of Ref. 25.

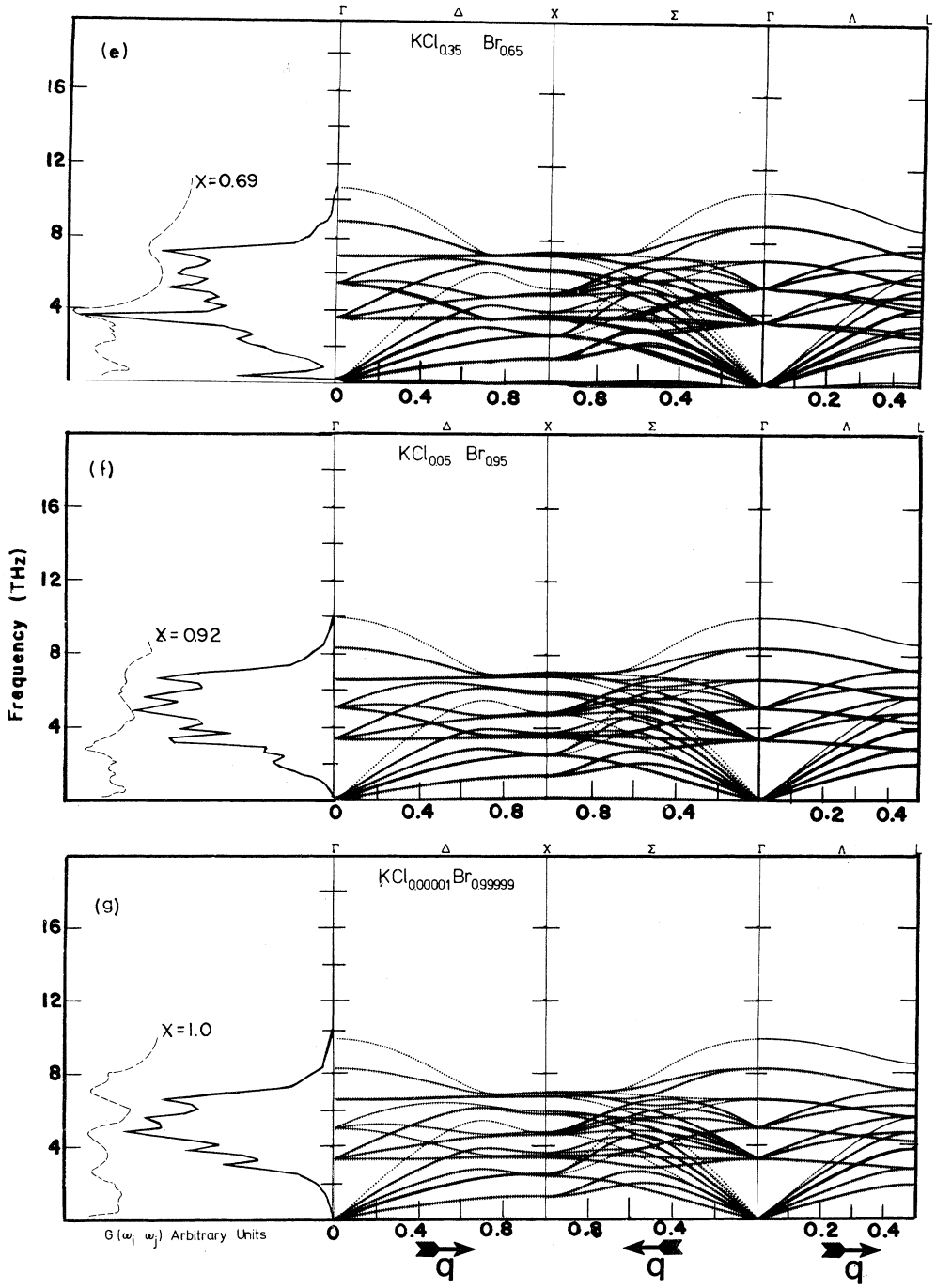

FIG. 5. (*Continued.*)

centration increases, the system becomes a ternary one that gives rise to an anomalous behavior in the acoustical modes at the zone center. Moreover, the longitudinal low-lying mode shows a kink related to the instability of this mode at certain molar fractions. Here, once more, one must stress the fact that the points shown in Fig. 3 are the actual calculated eigenvalues which implies that for a less dense mesh (say 30 points) most of these effects may go unnoticed. This instability can be easily

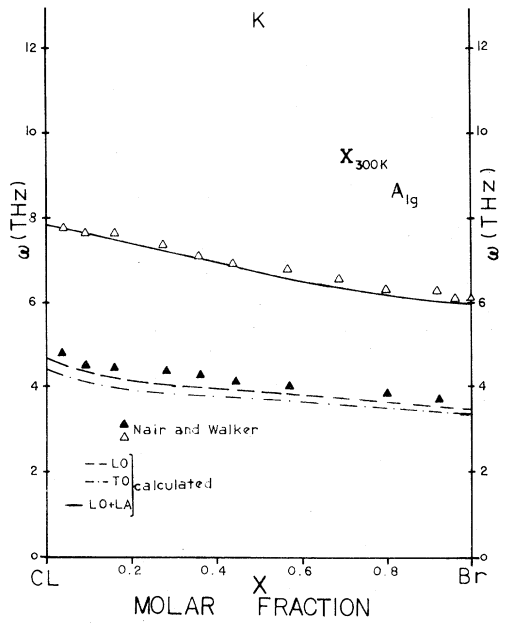

FIG. 6. Concentration dependence of phonons with A_{1g} symmetry of $KCl_{1-x}Br_x$.

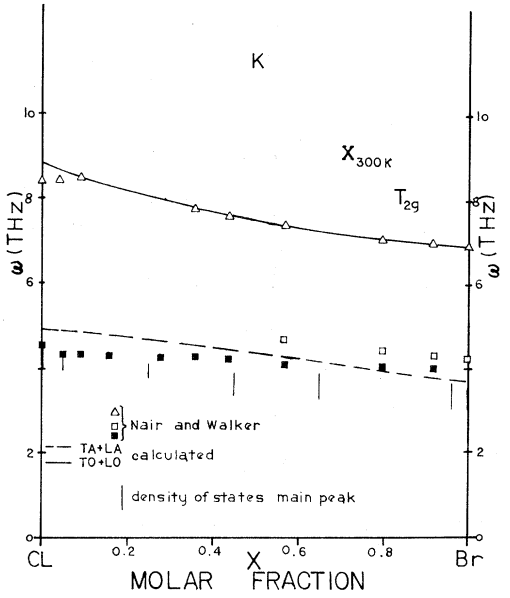

FIG. 7. Concentration dependence of phonons with T_{2g} symmetry of $KCl_{1-x}Br_x$.

made to disappear by increasing the effective ionic charge or by manipulating some of the force constants. This would involve an *ad hoc* explicit parametrization of the model without any clear physical meaning and without substantiating experimental data. Furthermore, this will not alter the basic dynamical results. Consequently, it was believed to be more useful to follow the evolution as the molar ratio changes. The result is as follows: The disturbance of the acoustic modes at the Γ point indicates that a maximum of instability for the longitudinal low-lying modes occurs at $x=0.50$.

At low temperatures the contribution to specific heat is predominantly from low-frequency phonons which belong to the acoustic branches at relatively long wavelengths. As can be seen in Fig. 3, densities of states show an anomalous peak at low frequencies whose presence will drastically change the bahavior of a thermal-expansion measurement. It is very interesting to note that such an effect has been measured, e.g., the case of a Li^+ impurity in KCl.[28] The low-lying modes contribute a large column at zero frequency to the histogram of density of states causing a distortion of the overall picture. We have therefore chosen to neglect the first small incremental step in frequency in the large peak.

Far-infrared measurements show a band at all concentrations studied. This implies that Kramer-Kronig analysis yields one longitudinal-optical mode and one transverse-optical mode characteristic of the one reststrahlen band. Figure 4 shows this result together with Refs. 9, 27, and 29. A possible explanation for the discrepancies is the uncertainty of the nature of the samples from which the experimental data have been obtained. Superimposed is the prediction of the pseudo-unit-cell model for Γ point that shows the right behavior with very good agreements at some concentrations.

A substantial impurity concentration will disrupt the translational symmetry and this will allow the otherwise forbidden first-order Raman peaks to be detected. Nair and Walker[25] have made an intensive experimental study of samples covering all molar ratios. It will be shown here that definitive conclusions can be drawn when the Raman spectra are compared with the results of the present calculation covering all molar ratios. Specimens analyzed in A_{1g} polarization geometry exhibit two main bands in the two-phonon region. Figures 5(a)—5(g) are the two-phonon lattice dynamics. Two-phonon densities of states are shown together

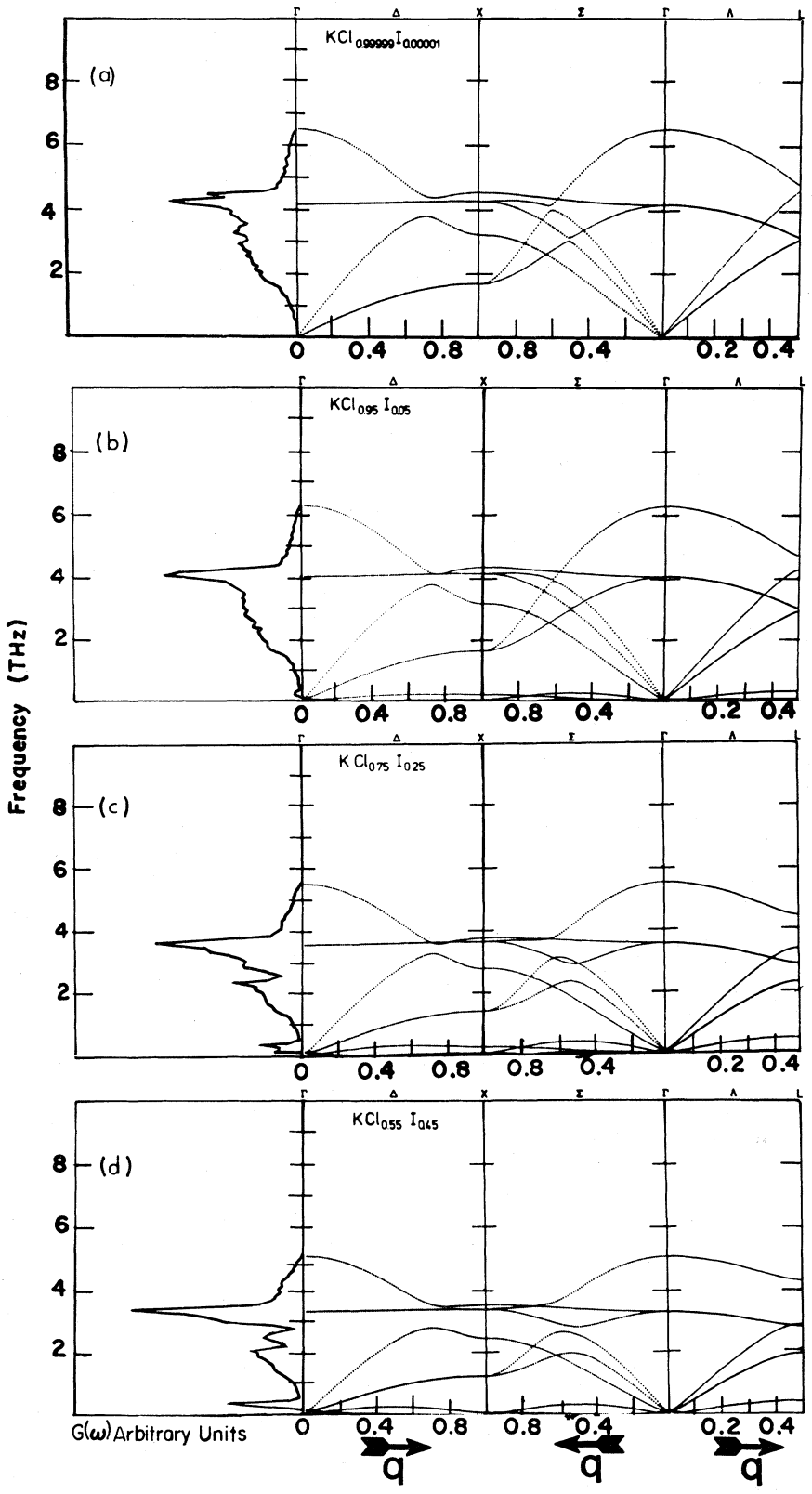

FIG. 8. One-phonon densities of states and dispersion relations of $KCl_{1-x}I_x$.

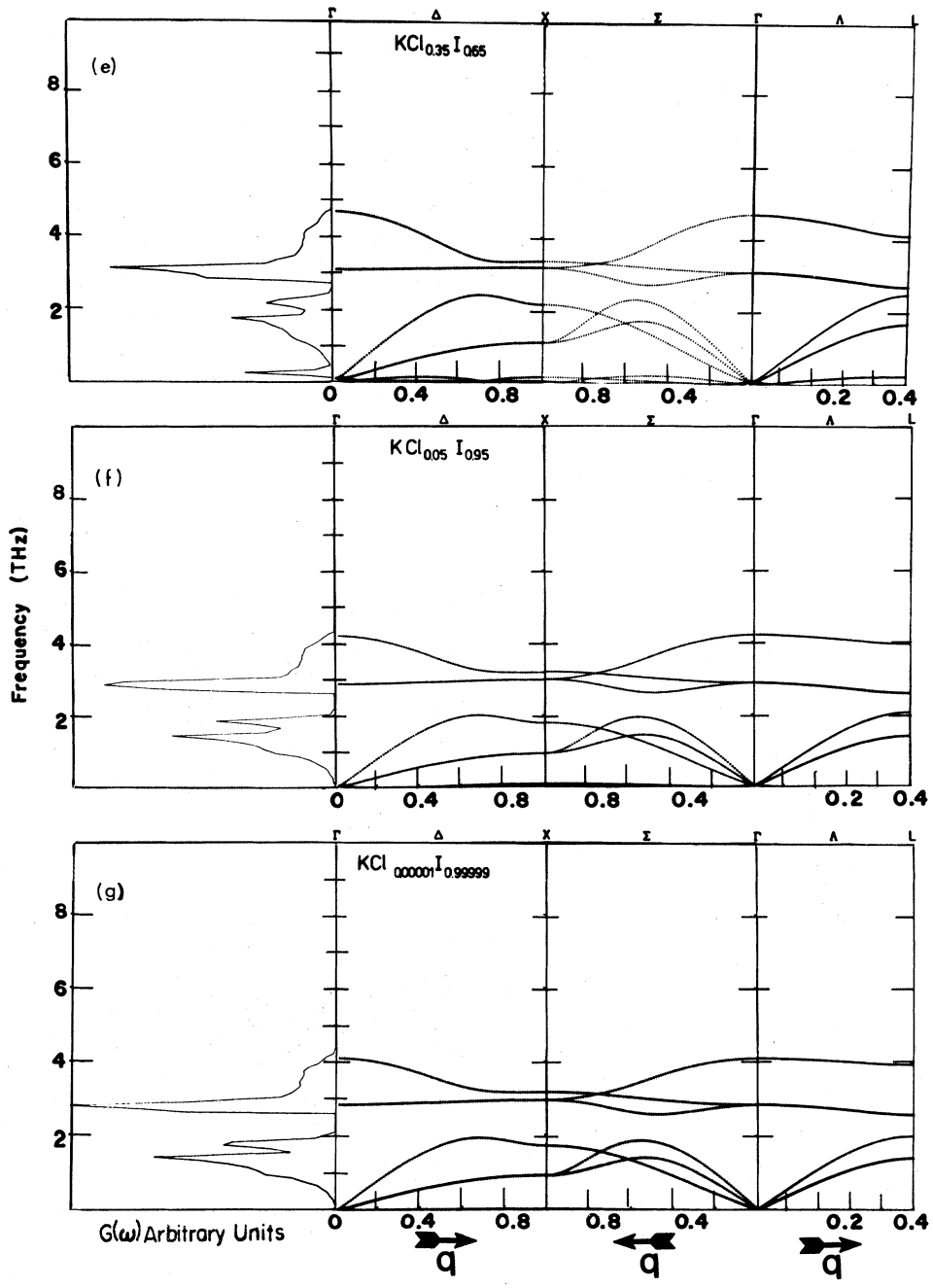

FIG. 8. (*Continued.*)

with the experimental results with nearest concentration ratios. From this is is seen that two-phonon Raman spectra of the two pure end members compare very well with the main features of the calculated two-phonon denstities of states at the lowest molar concentrations. It may also be pointed out that the band at about 8 THz can be assigned to the LO+LA combination. The low-frequency region can be assigned to one-phonon density of states as also was assumed by Nair and Walker for low concentrations and this seems to prevail at any molar ratio. This implies that from

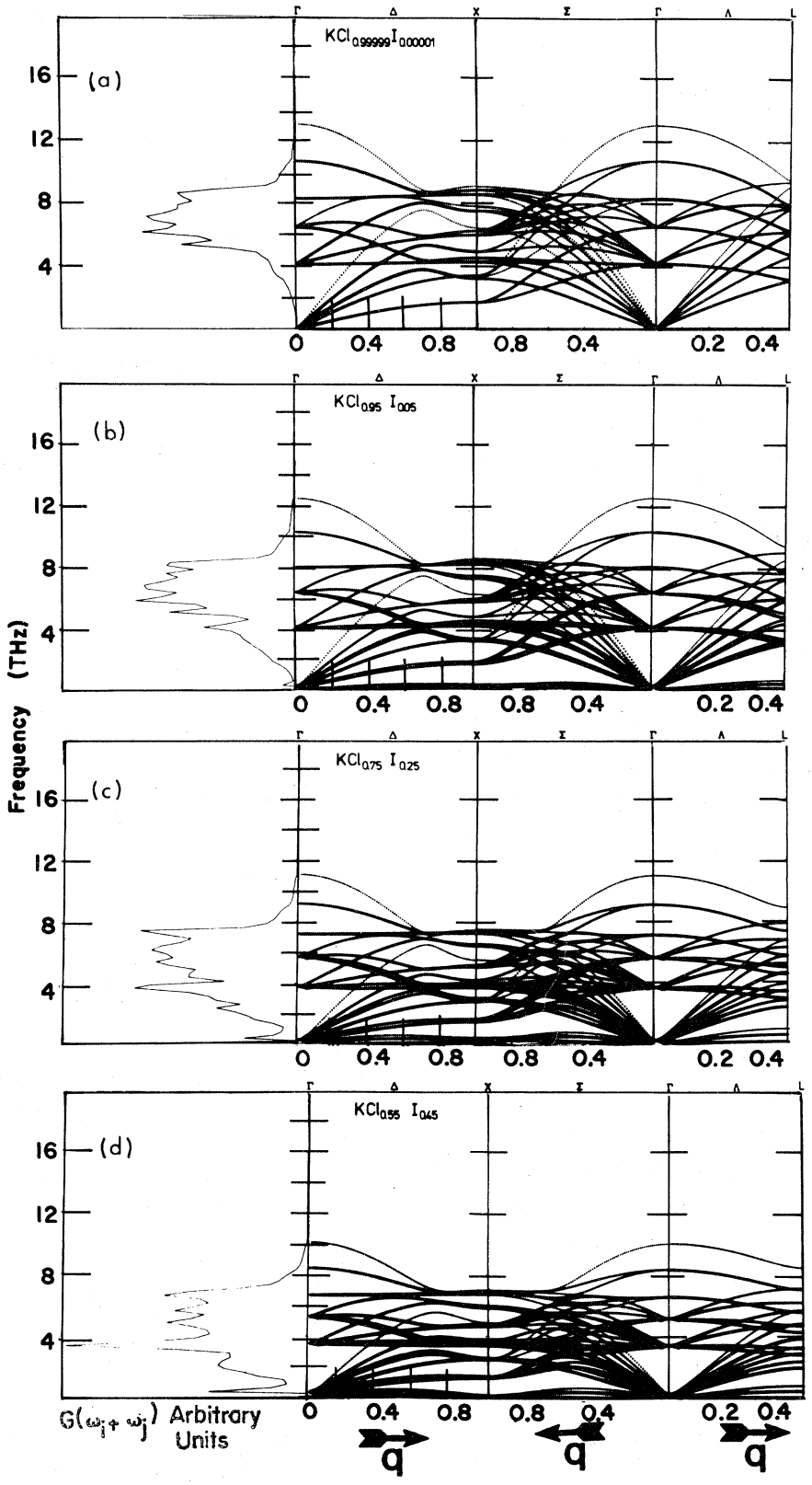

FIG. 9. Two-phonon densities of states and dispersion relations of $KCl_{1-x}I_x$.

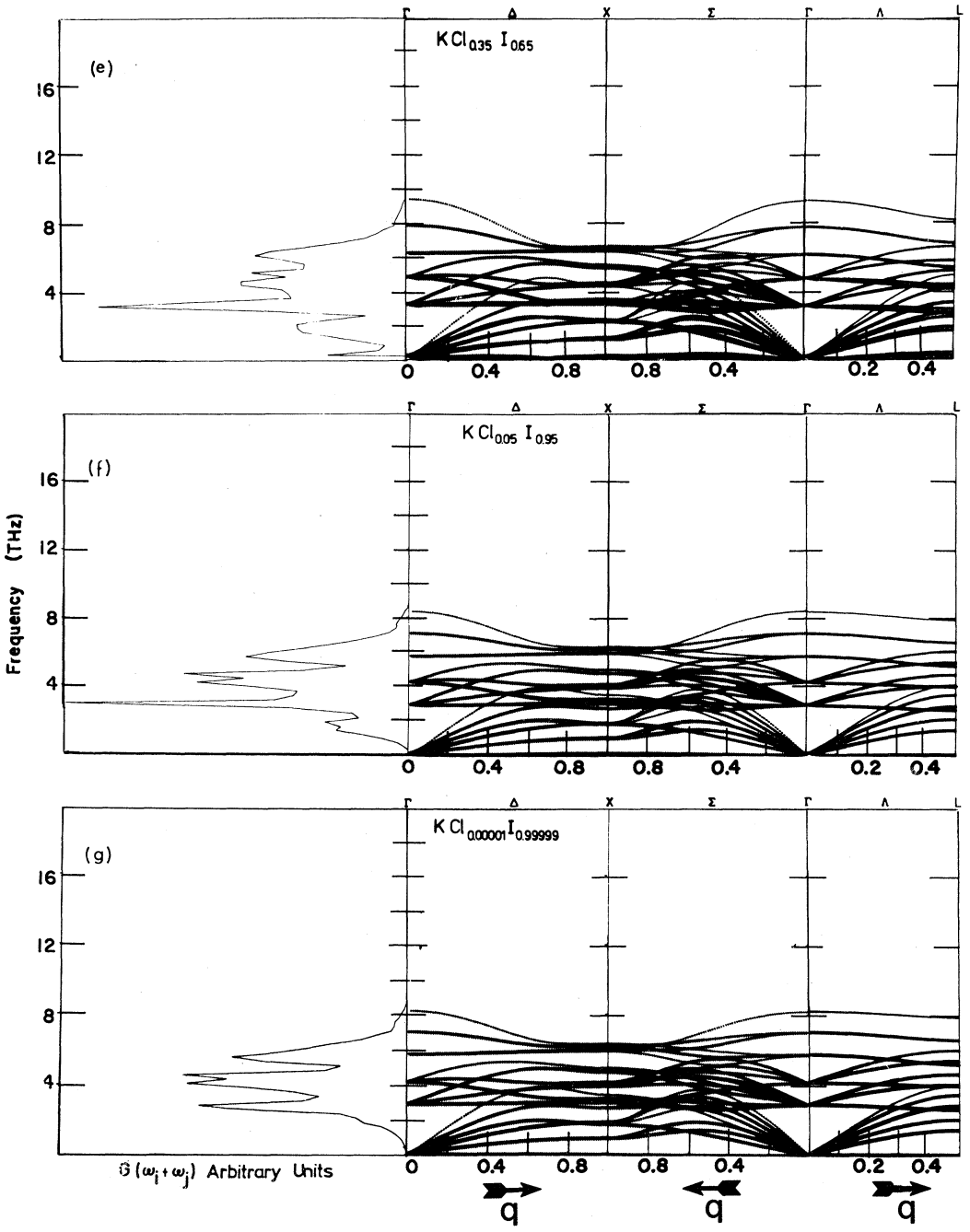

FIG. 9. (*Continued.*)

the Raman scattering data one is able to obtain a clear reflection of the phonon densities of states at any molar ratio. The correspondence between calculated and experimental peaks is almost one to one, particularly in the case of the acoustic bands.

To make these points even clearer, Fig. 6 shows the excellent agreement between the LO+LA assignment and the high-frequency peak, and the match of the calculated phonons, TO and LO at the X point with the main features of the one-

TABLE II. Short-range force constants and model parameters of $KCl_{1-x}I_x$.

$x =$	0.000 01	0.05	0.25	0.45	0.65	0.98	0.999 99	Units
A_{AB}	11.087	11.087	11.087	11.087	11.087	11.087	11.087	$e^2/2v$
A_{AC}	11.241	11.241	11.241	11.241	11.241	11.241	11.241	$e^2/2v$
A	11.087	11.094	11.125	11.156	11.187	11.233	11.241	$e^2/2v$
B_{AB}	−0.9228	−0.9228	−0.9228	−0.9228	−0.9228	−0.9228	−0.9228	$e^2/2v$
B_{AC}	−0.8817	−0.8817	−0.8817	−0.8817	−0.8817	−0.8817	−0.8817	$e^2/2v$
B	−0.9228	−0.9206	−0.9125	−0.9042	−0.8960	−0.8838	−0.8817	$e^2/2v$
A'_{AB}	-0.8512×10^{-1}	-0.8512×10^{-1}	-0.8512×10^{-1}	-0.8512×10^{-1}	-0.8512×10^{-1}	$-0.8512\times^{-1}$	-0.8512×10^{-1}	$e^2/2v$
A'_{AC}	−0.1251	−0.1251	−0.1251	−0.1251	−0.1251	−0.1251	−0.1251	$e^2/2v$
A'	-0.8512×10^{-1}	-0.8712×10^{-1}	-0.9512×10^{-1}	−0.1031	−0.1112	−0.1231	−0.1251	$e^2/2v$
B'_{AB}	-0.5507×10^{-4}	-0.5507×10^{-4}	-0.5507×10^{-4}	-0.5507×10^{-4}	-0.5507×10^{-4}	-0.5507×10^{-4}	-0.5507×10^{-4}	$e^2/2v$
B'_{AC}	-0.5328×10^{-4}	-0.5328×10^{-4}	-0.5328×10^{-4}	-0.5328×10^{-4}	-0.5328×10^{-4}	-0.4328×10^{-4}	-0.5328×10^{-4}	$e^2/2v$
B'	-0.5507×10^{-4}	-0.5498×10^{-4}	-0.5462×10^{-4}	-0.5427×10^{-4}	-0.5391×10^{-4}	-0.5337×10^{-4}	-0.5328×10^{-4}	$e^2/2v$
Z_{AB}	0.89	0.89	0.89	0.89	0.89	0.89	0.89	e
Z_{AC}	0.87	0.87	0.87	0.87	0.87	0.87	0.87	e
Z	0.889	0.888	0.885	0.881	0.877	0.871	0.87	e
Y_{AB}	−7.30	−7.30	−7.30	−7.30	−7.30	−7.30	−7.30	e
Y_{AC}	−6.71	−6.71	−6.71	−6.71	−6.71	−6.71	−6.71	e
Y	−7.30	−7.27	−7.15	−7.03	−6.91	−6.74	−6.71	e
k_{AB}	1573.24	1573.24	1573.24	1573.24	1573.24	1573.24	1573.24	$e^2/2v$
k_{AC}	1044.81	1044.81	1044.81	1044.81	1044.81	1044.81	1044.81	$e^2/2v$
k	1573.24	1546.82	1441.13	1335.45	1229.76	1071.24	1044.82	$e^2/2v$
G_{AB}	1041.93	1041.93	1041.93	1041.93	1041.93	1041.93	1041.93	$e^2/2v$
G_{AC}	1311.62	1311.62	1311.62	1311.62	1311.62	1311.62	1311.62	$e^2/2v$

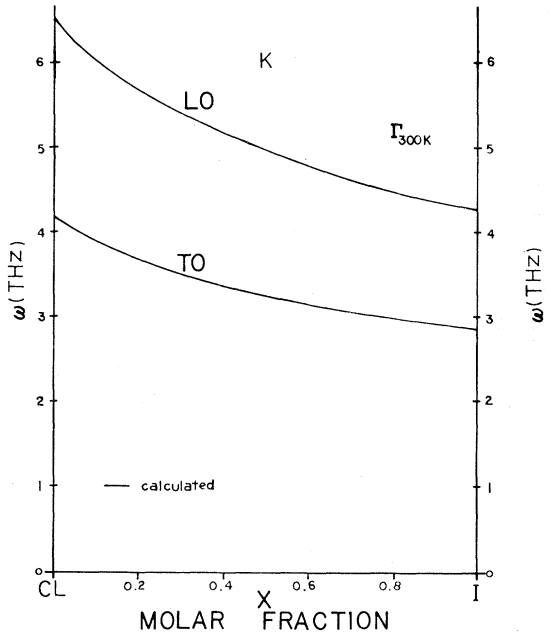

FIG. 10. Transerverse- and longitudinal-optical modes of $KCl_{1-x}I_x$.

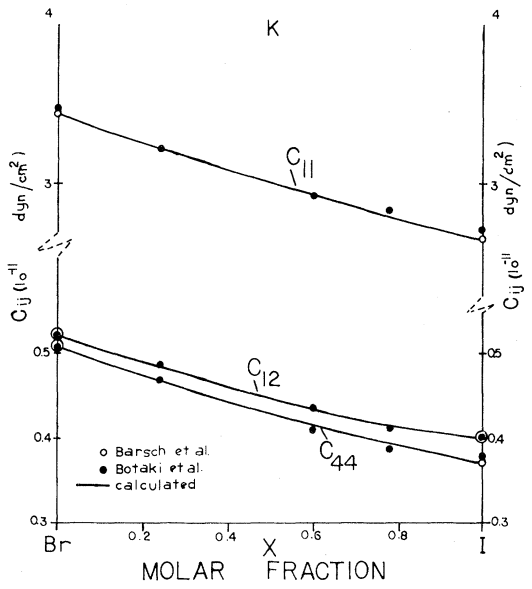

FIG. 11. Concentration dependence of the elastic constants of $KBr_{1-x}I_x$.

phonon region. These samples were also studied with the T_{2g} geometry. Once more a strong peak is observed in the one-phonon region (3—5 THz) and a broader, but well-defined band at higher frequencies (6—8 THz). The first is associated with the LA+TA summation in addition to processes associated with the combination of low-lying modes. However, the breakdown of selection rules imply also contributions from the entire density of states in addition to single summation processes indicated above that will result in a general broadening. For comparison we have also shown the half-width main peak position of the density of states in Fig. 7. It can also be seen that the band in the high-frequency side clearly corresponds to a LO(χ)+TO(χ) combination with contributions from 2TO(χ) and 2LO(χ) processes.

2. $KCl_{1-x}I_x$

Figures 8(a)—8(g) and 9(a)—9(g) show the complete lattice dynamics of these mixed crystals, assuming that they are miscible. Table II gives the force constants and parameters used in the calculation. Unfortunately, there is no infrared data, and only one composition has been studied by Nair and Walker[30] by Raman scattering. It was observed that for $x=0.04$ the acoustical band appears similar to the case discussed above. This is not surprising since KCl is still a well-defined host crystal for this concentration in which the presence of iodine ions excites the first-order spectra.

As in the case for $KCl_{1-x}Br_x$, Fig. 10 shows the position of longitudinal- and transverse-optical modes at the Γ point. The band due to the low-lying modes has a behavior similar to that described before, i.e., it goes to zero frequency as the concentration decreases, and has the maximum effect for $x=0.5$ in the distorted acoustic modes at the zone center.

3. $KBr_{1-x}I_x$

The elastic constants of this solid solution have been measured by Botaki *et al.*[31] at various concentrations. The assumption of linear additivity of the end-members force constants shown in Fig. 11 indicate, as in the case of $KCl_{1-x}Br_x$, a successful description of their molar-concentration dependence. $KBr_{1-x}I_x$ has been intensively studied in Ref. 30 using Raman scattering. Figures 12(a)—12(g) and 13(a)—13(g) show the one- and two-phonon spectra, calculated for all the concentration range, and the measured Raman spectra.

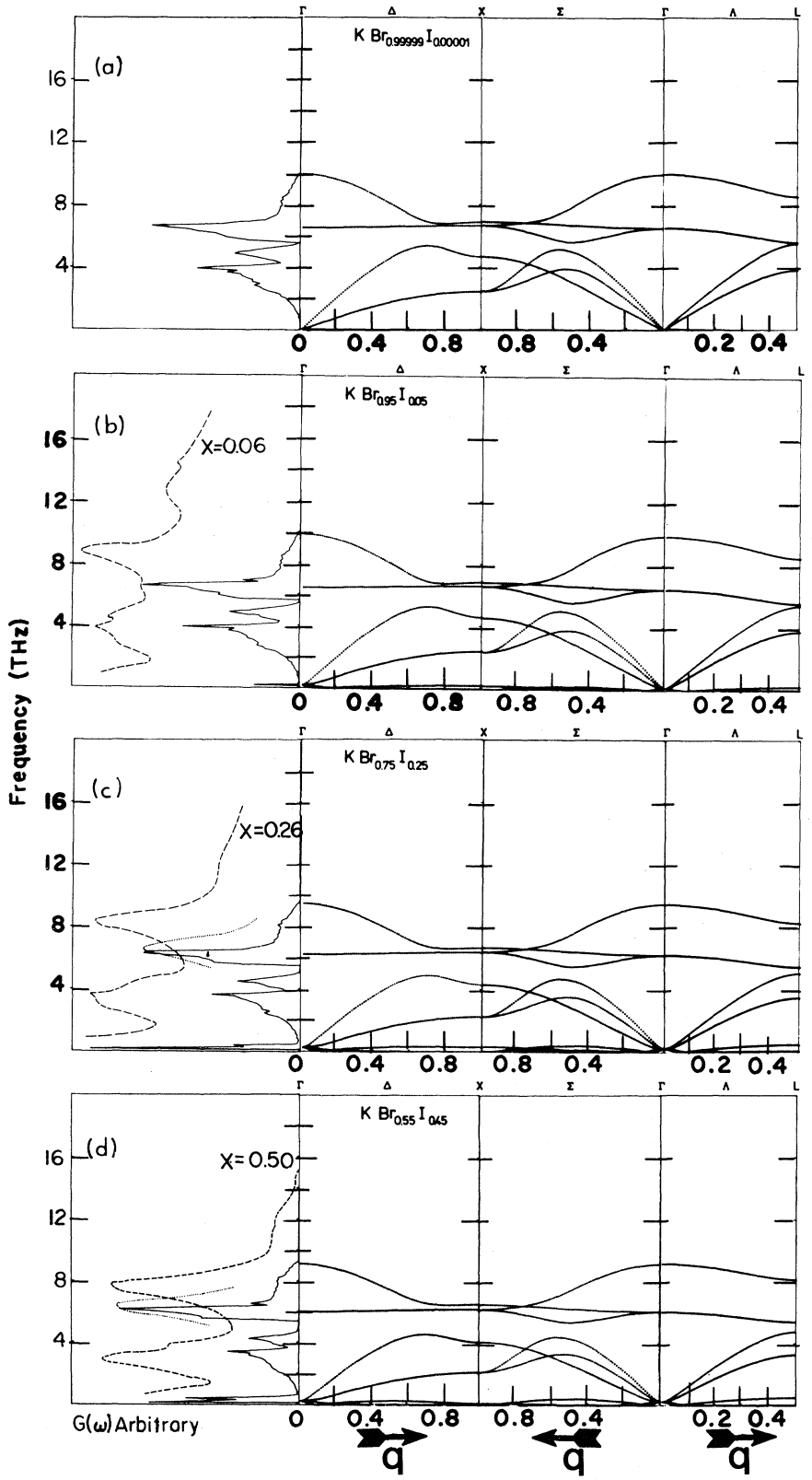

FIG. 12. One-phonon densities of states and dispersion relations of $KBr_{1-x}I_x$. Dashed lines correspond to Raman scattering results from Ref. 30. Dotted lines correspond to the corrected spectra due to the finite size of the samples.

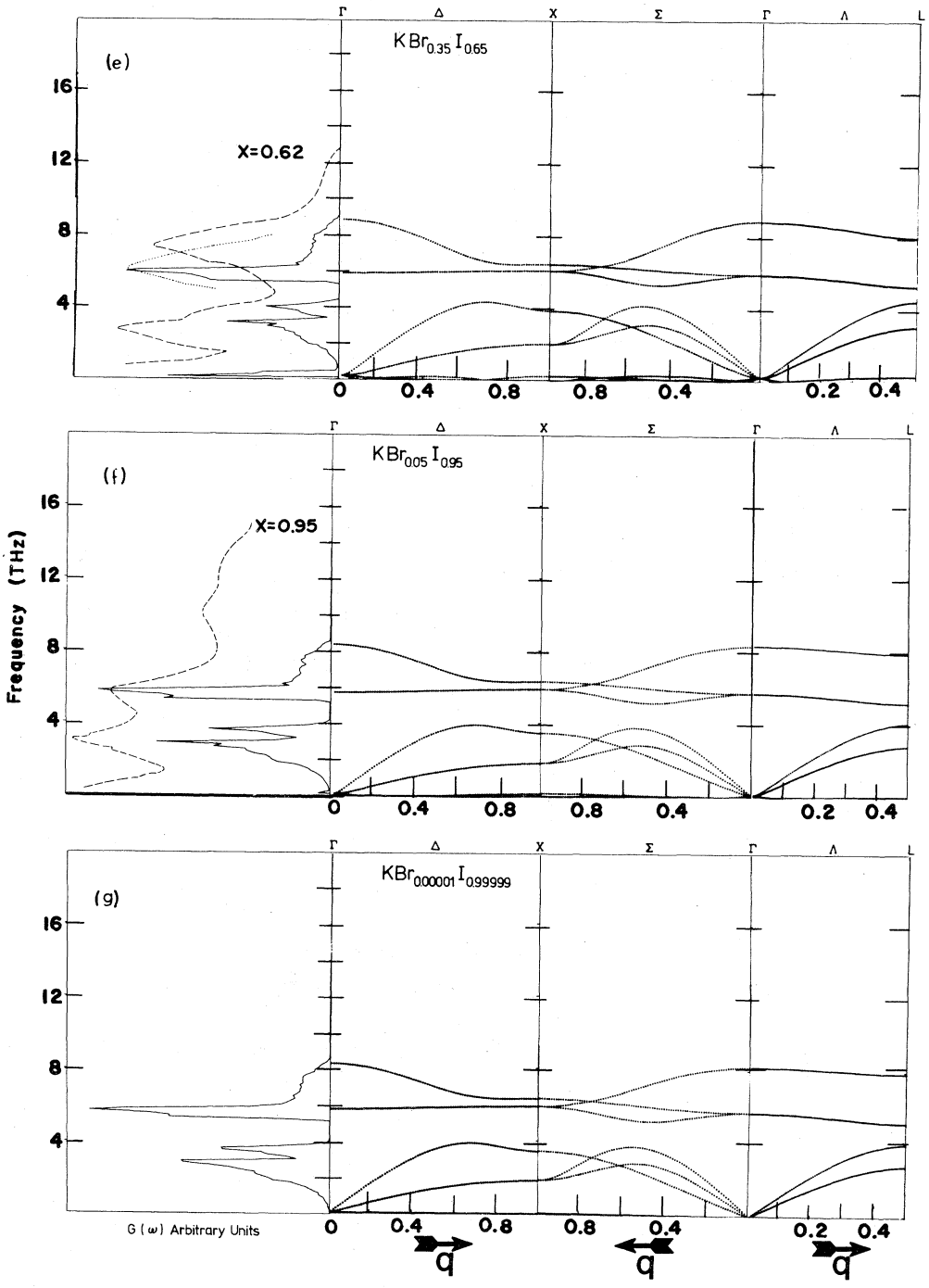

FIG. 12. (*Continued.*)

Figure 14 shows the predicted position of the infrared-active transverse and longitudinal modes. To date no infrared studies have been performed. Force constants and model parameters are shown in Table III. Experimentally the A_{1g} and T_{2g} symmetries have been studied showing similar features to those of the other two compounds discussed above. Figure 15 shows explicitly the assignment given to the higher frequency main band. As Figs. 12(a)—12(c) imply, rather than a single-phonon peak this band is more properly represented by a portion of the one-phonon density of states. This

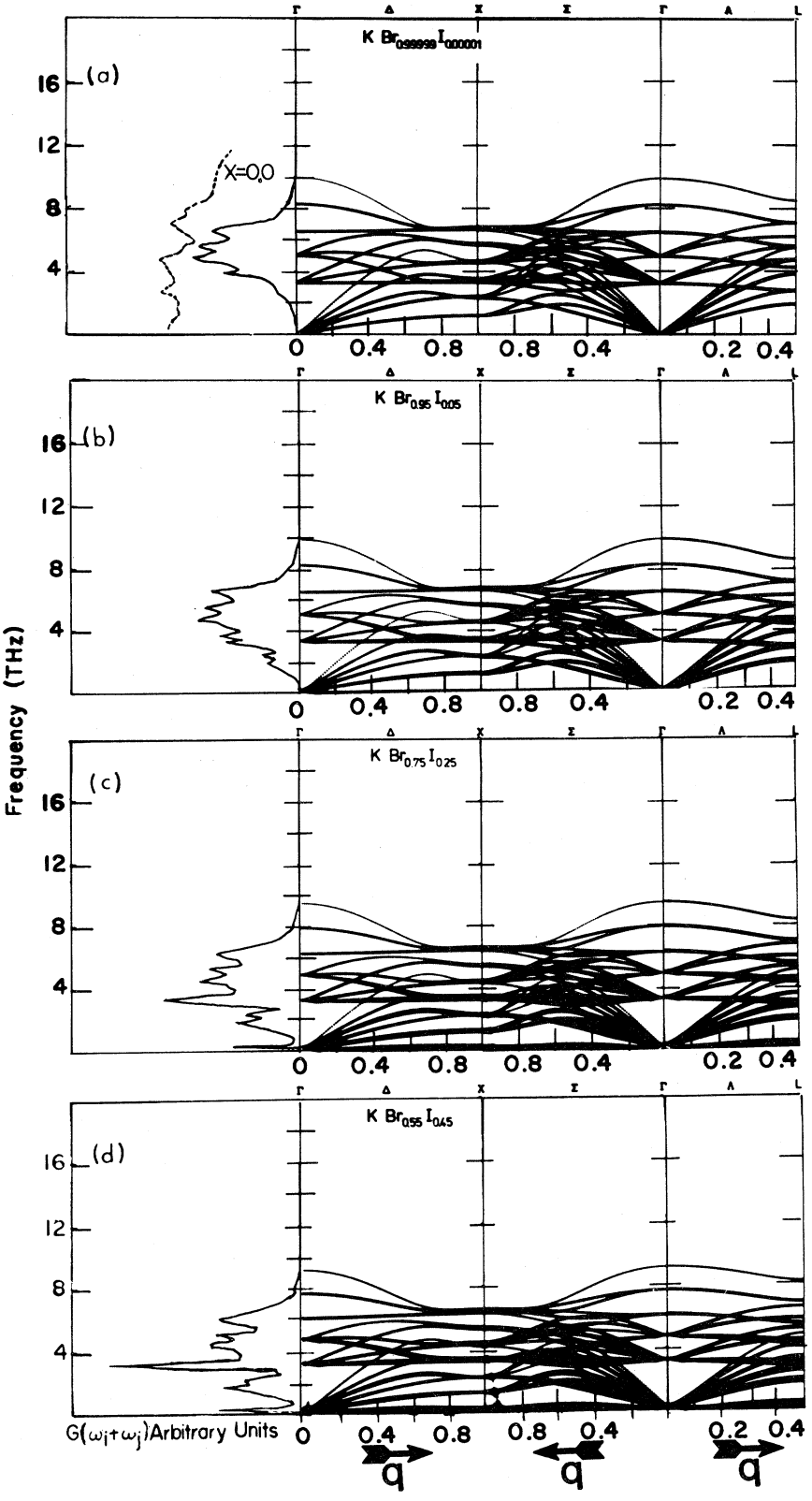

FIG. 13. Two-phonon densities of states and dispersion relations of $KBr_{1-x}I_x$. Dashed lines and inset correspond to Raman scattering results from Ref. 30.

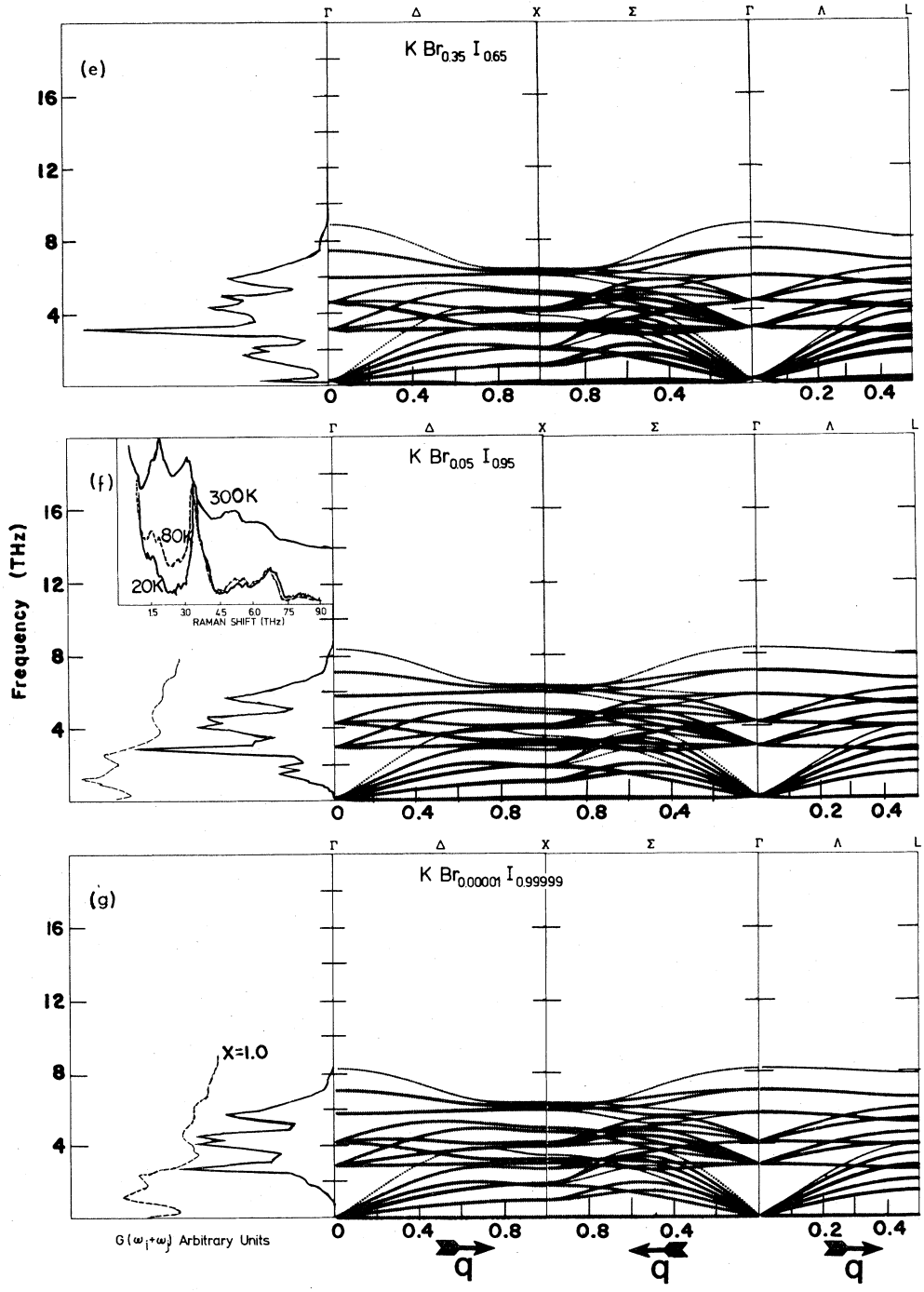

FIG. 13. (*Continued.*)

is also true for the lower part of the spectra.

Since TO and LO are the main contributors to the sharp peak at about 3.5 THz their positions have been plotted in Fig. 15 against the sample size corrected principal experimental A_{1g} peak. The same very good agreement is obtained when the lower frequency part of the spectrum is studied. Positions of LA(χ) and 2TA(χ) phonons have also been plotted against the experimental results. The reason for explicitly choosing an overtone band is

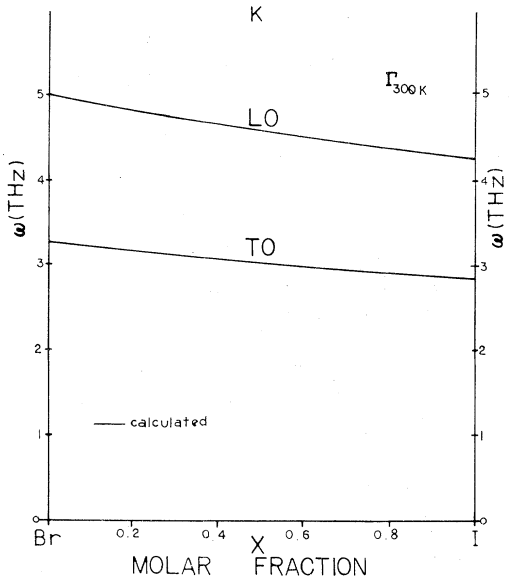

FIG. 14. Transverse- and longitudinal-optical modes to $KBr_{1-x}I_x$.

to make understood the role that first- and second-order peaks play in certain regions of the disordered spectrum. Main features in this region can always be associated to one-phonon but eventually the prominence of any band will be given by its electron-phonon interaction cross section. Another interesting feature to point out is the valley between peaks shown in Fig. 12 is much deeper than in the case of $KCl_{1-x}Br_x$, which indicates the presence of a gap in the one-phonon densities of states. A striking feature assigned in Ref. 30 as a first-order band for $x=0.95$ becomes understood when the spectrum is compared with two-phonon density of states. Figure 13(f) shows that the peak results from a LA+TA band and a combination of the low-lying modes with the optical modes. Then, a perfect match is obtained if the anharmonic temperature shift is taken into account. The low-intensity broadband in the high-frequency side of the inset can be seen to correspond correctly to the combination bands of the two-phonon density of states. The spectrum of T_{2g} symmetry shows a feature that apparently is the superposition of at least two main structures associated with the acoustic bands and the low-lying modes. Figure 16 shows the experimental points against LA+TA, at the L and X symmetry points, as functions of the molar ratio. This is related to the strong peak observed with A_{1g} symmetry and it is consistent, since it is a second-order feature, with the fact that it remains detectable even in the pure end compound. Figure 16 also shows the half-width position of the main band of the calculated one-phonon density of states. This is to point out, as in the case of $KCl_{1-x}Br_x$, the contribution of the first-order processes to the lower-frequency part of the spectra.

V. SUMMARY AND CONCLUSIONS

The lattice dynamics of one-mode-behavior mixed alkali-halide crystals with negative-ion substitution has been discussed under a pseudo-unit-cell approach. This technique simulates a topological average with regard to the locations of ions in lattice. A repetitive unit for $AB_{1-x}C_x$ compound is a cell consisting of A ions at their normal lattice site and with nearest neighbors consisting of a fractional amount of B and C proportional to their mixing molar ratio. The basic lattice-dynamics model employed is the breathing-shell model in which positive ions are assumed to consist of hard cores only, while negative ions consist of hard cores and deformable shells. The model parameters were deduced from physical observables of the end systems. Short- and long-range coupling coefficients were weighted by molar fraction factors that depend on the concentration of the appropriate interacting ions.

One- and two-phonon dispersion relations and density of states have been calculated for $KCl_{1-x}Br_x$, $KCl_{1-x}I_x$, $KBr_{1-x}I_x$. One may infer that the common denominator for one-mode mixed crystal with negative substitution corresponds to the appearance of a low-frequency band perturbing the acoustical modes at the zone center. It would behave as a kind of impurity "soft mode" and it goes to zero frequency when the impurity is reduced to minimum levels. Optical and acoustical bands have an overall very good agreement with what was observed experimentally. This implies a strong support for the proposed model since experimental peaks of the Raman spectra of the distorted system are always associated with higher symmetry points. Thus a logical conclusion that a pseudo-Brillouin-zone still exists, regardless of the molar ratio. This will have the crystalline symmetry points but with relaxed selection rules associated with them, further supporting the concept of a three-dimensional pseudo-unit-cell, and by extension, the pseudo-Brillouin-zone in the reciprocal space.

The authors want to point out that they are will-

TABLE III. Short-range force constants and model parameters of $KBr_{1-x}I_x$.

$x=$	0.0001	0.05	0.25	0.45	0.65	0.95	0.999 99	Units
A_{AB}	11.087	11.087	11.087	11.087	11.087	11.087	11.087	$e^2/2v$
A_{AC}	10.898	10.898	10.898	10.898	10.898	10.898	10.898	$e^2/2v$
A	11.087	11.077	11.039	11.002	10.964	10.907	10.898	$e^2/2v$
B_{AB}	−0.9228	−0.9228	−0.9228	−0.9228	−0.9228	−0.9228	−0.9228	$e^2/2v$
B_{AC}	−0.8817	−0.8817	−0.8817	−0.8817	−0.8817	−0.8817	−0.8817	$e^2/2v$
B	−0.9228	−0.9207	−0.9125	−0.9042	−0.8960	−0.8838	−0.8817	$e^2/2v$
A'_{AB}	-0.8512×10^{-1}	-0.8512×10^{-1}	-0.8512×10^{-1}	-0.8512×10^{-1}	-0.8512×10^{-1}	-0.8512×10^{-1}	-0.8512×10^{-1}	$e^2/2v$
A'_{AC}	-0.3145×10^{-1}	-0.3145×10^{-1}	-0.3145×10^{-1}	-0.3145×10^{-1}	-0.3145×10^{-1}	-0.3145×10^{-1}	-0.3145×10^{-1}	$e^2/2v$
A'	-0.8512×10^{-1}	-0.8243×10^{-1}	-0.7170×10^{-1}	-0.6069×10^{-1}	-0.5023×10^{-1}	-0.3413×10^{-1}	-0.3145×10^{-1}	$e^2/2v$
B'_{AB}	-0.5507×10^{-4}	-0.5507×10^{-4}	-0.5507×10^{-4}	-0.5507×10^{-4}	-0.5507×10^{-4}	-0.5507×10^{-4}	-0.5507×10^{-4}	$e^2/2v$
B'_{AC}	-0.5334×10^{-4}	-0.5334×10^{-4}	-0.5334×10^{-4}	-0.5334×10^{-4}	-0.5534×10^{-4}	-0.5334×10^{-4}	-0.5334×10^{-4}	$e^2/2v$
B'	-0.5507×10^{-4}	-0.5499×10^{-4}	-0.5464×10^{-4}	-0.5429×10^{-4}	-0.5395×10^{-4}	-0.5343×10^{-4}	-0.5334×10^{-4}	$e^2/2v$
Z_{AB}	0.89	0.89	0.89	0.89	0.89	0.89	0.89	e
Z_{AC}	0.87	0.87	0.87	0.87	0.87	0.87	0.87	e
Z	0.889	0.888	0.885	0.881	0.877	0.871	0.87	e
Y_{AB}	−7.30	−7.30	−7.30	−7.30	−7.30	−7.30	−7.30	e
Y_{AC}	−6.76	−6.76	−6.76	−6.76	−6.76	−6.76	−6.76	e
Y	−7.30	−7.273	−7.165	−7.057	−6.949	−6.787	−6.76	e
k_{AB}	1573.24	1573.24	1573.24	1573.24	1573.24	1573.24	1573.24	$e^2/2v$
k_{AC}	1209.90	1209.90	1209.90	1209.90	1209.90	1209.90	1209.90	$e^2/2v$
k	1573.24	1555.07	1482.41	1409.74	1337.07	1222.07	1209.90	$e^2/2v$
G_{AB}	1041.93	1041.93	1041.93	1041.93	1041.91	1041.93	1041.93	$e^2/2v$
G_{AC}	4815.47	4815.47	4815.47	4815.47	4815.47	4815.47	4815.47	$e^2/2v$

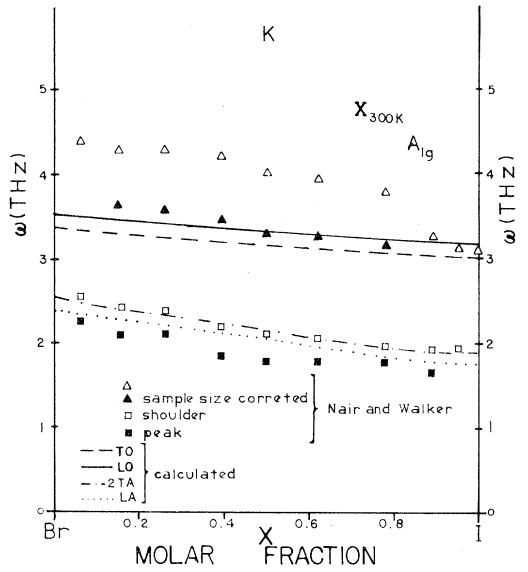

FIG. 15. Concentration dependence of phonons with A_{1g} symmetry of $KBr_{1-x}I_x$.

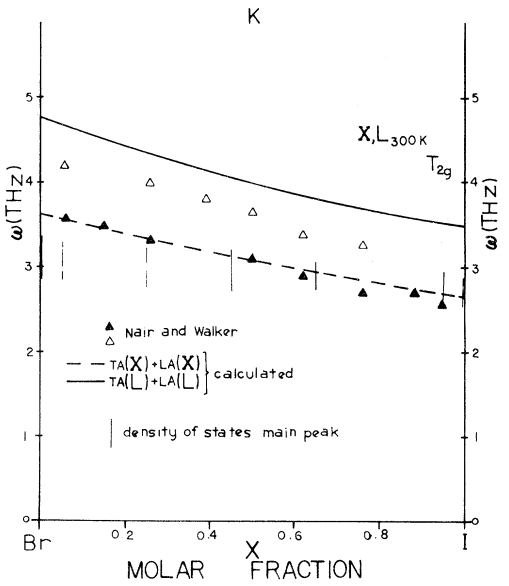

FIG. 16. Concentration dependence of phonons with T_{2g} symmetry of $KBr_{1-x}I_x$.

ing to provide upon request the calculated eigenvalues of the dispersion curves and the corresponding density of states from the on-line computer output for any molar concentration and mixed crystal presented in this paper.

ACKNOWLEDGMENTS

The authors are pleased to acknowledge the financial support from the National Science Foundation to the Academic Computer Center of the University of Rhode Island, where all the calculations were made. One of us (N.E.M.) wants to extend thanks to Professor John R. Hardy (University of Nebraska, Lincoln) for reading the manuscript and to acknowledge the hospitality of the Department of Electrical Engineering and the Department of Physics at the University of Rhode Island during his stay at U.R.I.

[1]L. Vegard, Z. Phys. 5, 17 (1921).
[2]H. C. Poon and A. Bienenstock, Phys. Rev. 141, 710 (1966); 142, 466 (1966).
[3]I. Chang and S. S. Mitra, Adv. Phys. 20, 359 (1971).
[4]A. S. Barker, Jr. and A. J. Sievers, Rev. Mod. Phys. 47, Suppl. 2, S1–S179 (1975).
[5]Y. S. Chen, W. Shockley, and G. L. Pearson, Phys. Rev. 151, 648 (1966).
[6]I. F. Chang and S. S. Mitra, Phys. Rev. 172, 924 (1968).
[7]L. Genzel, T. P. Martin, and C. H. Perry, Phys. Status Solidi B 62, 83 (1974).
[8]E. Jahne, Phys. Status Solidi B 74, 275 (1976); 75, 221 (1976).
[9]J. H. Fertel and C. H. Perry, Phys. Rev. 184, 874 (1969).
[10]L. Genzel, T. P. Martin, and C. H. Perry, Phys. Status Solidi B 62, 83 (1974).
[11]A. P. G. Kutty, Solid State Commun. 14, 213 (1974).
[12]R. S. Tripathi and S. N. Behera, J. Phys. C 7, 4470 (1974); also, S. N. Behera and R. S. Tripathi, *ibid.* 7, 4452 (1974).
[13]R. I. Elliott, J. A. Krumhouse, and P. L. Leath, Rev. Mod. Phys. 46, 465 (1974).
[14]D. W. Taylor, Solid State Commun. 13, 117 (1973); (unpublished).
[15]P. N. Sen and W. M. Hartmann, Phys. Rev. B 9, 367 (1974).
[16]I. F. Chang, Ph.D. dissertation, University of Rhode Island, 1968 (unpublished).

[17]J. F. Vetelino and S. S. Mitra, in *Physics of Structurally Disordered Solids,* edited by S. S. Mitra (Plenum, New York, 1976), p. 541.
[18]S. C. Varshney, J. F. Vetelino, S. S. Mitra, and I. F. Chang, Phys. Rev. B 12, 5912 (1975).
[19]M. Born and K. Huang, *Dynamical Theory of Crystal Lattices* (Oxford University Press, Oxford, 1954), p. 217.
[20]W. Bauhofer and L. Genzel, Phys. Status Solidi 62, 361 (1974).
[21]H. Bilz, Summer Institute in Physics, Freiburg, Germany, 1966 (unpublished).
[22]U. Schroeder, Solid State Commun. 4, 347 (1966).
[23]O. D. Slagle and H. A. McKinstry, J. Appl. Phys. 38, 446 (1967); see also, L. S. Cain, J. Phys. Chem. Solids 37, 1178 (1976).
[24]A. V. Sharko and A. A. Botaki, Izv. Vyssh. Uchebn. Zaved. Fiz. 12, 126 (1971) [Sov. Phys. J. 14, 1710 (1971)].
[25]I. Nair and C. T. Walker, Phys. Rev. B 3, 3346 (1971).
[26]J. H. Fertel and C. H. Perry, Phys. Lett. 36A, 315 (1971).
[27]J. R. Ferraro, C. Postmus, S. S. Mitra, and C. J. Hoskins, Appl. Opt. 9, 5 (1970).
[28]C. R. Case, K. O. McLean, C. A. Swenson, and G. K. White, in *Thermal Expansion—1971 (Corning),* Proceedings of the 1971 Thermal Expansion Symposium, edited by M. C. Graham and H. E. Hagy (AIP, New York, 1971), p. 183.
[29]A. Mitsuishi, presented at U.S.—Japan Cooperative Seminar on Far Infrared Spectroscopy, Columbus, Ohio, 1965 (unpublished), as quoted by Chang and Mitra, Adv. Phys. 20, 359 (1971). For low-temperature measurements see J. F. Angress, G. A. Giedpull, and J. D. Clark, in *Lattice Dynamics,* edited by B. M. Balkanski (Flammarion, Paris, 1977).
[30]I. Nair and C. T. Walker, Phys. Rev. B 7, 2740 (1973).
[31]A. A. Botaki, I. N. Gyrbu, and A. V. Sharko, Izv. Vyssh. Uchebn. Zaved. Fiz. 6, 150 (1972) [Sov. Phys. J. 15, 917 (1972)].